DOI: 10.1002/ejic.201001055

A Decade of Octacyanides in Polynuclear Molecular Materials

Barbara Sieklucka,*[a] Robert Podgajny,[a] Tomasz Korzeniak,[a] Beata Nowicka,[a] Dawid Pinkowicz,[a] and Marcin Koziel[a]

Keywords: Cyanides / Heterometallic complexes / Crystal engineering / Solid-state structures / Structure–acivity relationships

The aim and the scope of this review is to show the results of ten years of research following the first reports on magnetic and photomagnetic assemblies constructed from $[M(CN)_8]^{n-}$. It is illustrated on the basis of our own work as well as a wide range of studies carried out in numerous laboratories around the world. The diversity and evolution of topological and structural patterns is discussed alongside synthetic strategies, which led to the establishment of regular magnetostructural correlations in selected 3D systems. Different types of functionality observed in solid phases are presented with special attention devoted to tuning of magnetic properties by physical and chemical stimuli. Examples of advanced properties discovered in octacyanometallate-based magnetic materials comprise SMMs (single molecule magnets) and SCMs (single chain magnets), nonlinear effects MSHG (magnetization-induced second harmonic generation) and chirality, SCO (spin crossover) and luminescence. The potential of the development of octacyanometallate-based coordination assemblies towards addressable, multifunctional molecular materials for future application is discussed.

1. Introduction

The interest in the development of new functional materials has stimulated extensive research into synthesis of polynuclear complexes and attempts at their rational design, which intensified in the last decade. The combination of single molecular components bearing specific structural properties (shape, connectivity, symmetry, rigidity/flexibility), electronic properties (HOMO and LUMO energy levels, chemical reactivity including coordination and redox reactivity, unpaired electrons, magnetic anisotropy) and optical properties (absorption, emission and conversion of energy) led to a variety of novel coordination assemblies, which combine the phenomena characteristic for traditional inorganic and organic materials: magnetic ordering, energy conversion, nonlinear optical properties, chirality, conductivity or physisorption and chemisorption of guest molecules in gas–solid and liquid–solid biphasic systems.[1] Significant progress was noted in some of these fields, which included trapping and observing the chemical species in different stable or metastable states (structural, electronic, magnetic) at specific conditions as well as reversible thermal, light, pressure, magnetic and chemical switching between these states.[2] Among the most appealing coordination species are MOF-type[3] and MIL-type[4] (MIL = Materials of Institut Lavoisier) networks, acentric[5] and chiral[6] networks, SMMs[7] and SCMs,[8] single magnetic domain species, SCO systems[9] and magnetically ordered networks[10] with tuneable T_c temperatures.

The great interest in octacyanometallate-bridged assemblies followed directly the wealth of compounds based on lower coordination number polycyanometallates: Cu^I-, Ag^I-, Au^I-based networks with linear or triangle connectors, Cu^I- or Zn^{II}-based networks of tetrahedral connectors, clay-like layered $[M'(CN)_4M'']\cdot n$guest species with square-like nodes, cubic Prussian blue analogues and $[Mo(CN)_7]^{4-}$- and $[Re(CN)_7]^{3-}$-based compounds.[9,10a,10b,11] While stemming originally from the field of inorganic coordination chemistry, the design and synthetic routes toward novel networks quickly started to adapt the organic components of potential to act as blocking ligands, bridging ligands, counterions or separate molecular building blocks, which played a crucial role in the design of topology, dimensionality and the resulting properties.

Before 2000, relatively few articles referring to $[M(CN)_8]^{n-}$ compounds were published. Reported for the first time in 1904, successively studied and characterized during the last century, they were of interest mainly from the point of view of their redox reactivity and ability to form mixed valence species. The historical overview together with the basic characterization and earlier results on octacyanometallate-based bimetallic networks were presented in our previous reviews.[12] Since 2000 there has been a rapid increase in the number of papers related to crystal structure and different functionalities of polynuclear octacyanometallate-

[a] Faculty of Chemistry, Jagiellonian University, Ingardena 3, 30-060 Kraków, Poland

bridged assemblies (Figure 1). The outburst began with the report on the hexanuclear cluster $[Mn^{II}(bpy)_2][M^{IV}(CN)_8]\cdot 8H_2O$ (M = Mo, W) having an octahedral cyanide-bridged skeleton protected by four sets of bpy ligands (Figure 2a),[13] shortly followed by the first examples of high-spin clusters $\{Mn^{II}_9[M^{V}(CN)_8]_6(solv)_{24}\}\cdot x$solv (M = Mo, W; solv = MeOH or EtOH)[14,15] (Figure 2b) and 3D magnetically ordered networks.[16,17]

These first spectacular results were succeded by numerous reports, many of which constituted valuable contributions to contemporary magnetochemistry. The synthesis of an original family of soft magnets based on a 2D bilayered $\{Cu^{II}[M^{V}(CN)_8]^-\}_n$ backbone with a T_c of 28–40 K and strong magnetic anisotropy[18] stimulated thorough structural, magnetic and calorimetric characterization of this type of assemblies.[19] The first mixed organic–inor-

Barbara Sieklucka is a full Professor of Inorganic Chemistry at the Jagiellonian University, the head of the Inorganic Molecular Materials Group and a cofounder of the European Institute of Molecular Magnetism. She is the author of numerous contributions in coordination chemistry and molecular magnetism and an expert on octacyanometallate chemistry. Her current research interests include the development of cyanide-bridged bimetallic assemblies into multifunctional magnetic molecular materials.

Dr Robert Podgajny received his PhD from the Jagiellonian University in 2002. He developed his skills in molecular magnetism at the P. & M. Curie University in Paris and in handling metallic nanoparticles in LCC CNRS in Toulouse (France). His area of expertise involves crystal engineering of magnetic coordination networks. He is now developing methods of construction of molecular materials using high-spin secondary building blocks.

Dr Tomasz Korzeniak obtained his PhD from the Jagiellonian University in 2005. He did his post-doc research at the Institute for Molecular Science in Valencia (Spain), studying linkage isomerism in Prussian blue analogues. His current scientific interests concern the design and functionality of cyanide-bridged hybrid networks.

Dr Beata Nowicka completed her PhD in coordination chemistry at the Jagiellonian University in 1998. She gained experience in the synthetic chemistry laboratories at the University of Erlangen-Nürnberg in Germany and the Institute of Physical and Chemical Research (RIKEN) in Japan. In 2005 she joined the Inorganic Molecular Materials Group and now works on guest-responsive porous magnetic networks.

Dr Dawid Pinkowicz has just finished his PhD and obtained a European Doctorate in Molecular Magnetism diploma issued by the European Institute of Molecular Magnetism. During his thesis he spent a year at the Laboratory of Molecular Magnetism, University of Florence (Italy). His research focuses on switchable magnetic materials showing topotactic reactivity.

Marcin Kozieł is a PhD student in the Inorganic Molecular Materials Group. His main interest concerns 4f–5d magnetic coordination networks. He also studies the photomagnetic effect in bimetallic materials in cooperation with CNRS and the Universities of Bordeaux and Toulouse (France).

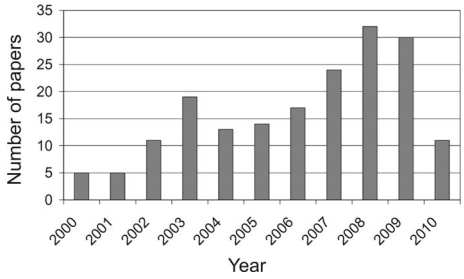

Figure 1. Diagram showing the increasing interest in octacyanometallate-based coordination assemblies during the last decade.

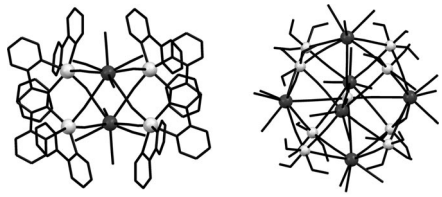

Figure 2. The first octacyanometallate-based clusters: (a) $\{[Mn^{II}(bpy)_2][M^{IV}(CN)_8]\}$ (M = Mo, W) and (b) $\{Mn^{II}_9[M^{V}(CN)_8]_6(solv)_{24}\}$. Dark grey spheres: Mo, W; light grey spheres: 3d metals; black sticks: CN^- bridges and blocking ligands.

ganic hybrid network, $[Cu(\mu\text{-}4,4'\text{-bpy})(dmf)_2][Cu(\mu\text{-}4,4'\text{-bpy})(dmf)]_2[W^{V}(CN)_8]_2\cdot 2dmf\cdot 2H_2O$,[20] was obtained, and the photomagnetic properties of $[Mn^{II}(bpy)_2][M^{IV}(CN)_8]\cdot 8H_2O$ clusters were studied.[21] Thanks to the discovery of magnetostructural correlations in structurally related compounds, different methods for tuning T_c were achieved: (1) by changing divalent 3d metal cations in $\{[M'^{II}(pyrazole)_4]_2[Nb^{IV}(CN)_8]\cdot 4H_2O\}_n$ (Mn^{II}, Fe^{II}, Co^{II} or Ni^{II}) series,[22] (2) by replacing organic ligands in $\{Mn^{II}\text{–}L\text{–}Nb^{IV}(CN)_8\}_n$ (L = pyz, 4,4′-pzdo, ImH, bpym and urea) networks[23] and (3) by sorption/exchange of small solvent molecules in 2D $\{[Ni^{II}(cyclam)]_3[W^{V}(CN)_8]_2\}_n\cdot x$solv[24] and 3D $\{Mn^{II}\text{–}L\text{–}Nb^{IV}(CN)_8\}$ (L = ImH, urea).[23c,25] Among the most important achievements, we count the acentric chiral network $\alpha\text{-}\{[Mn^{II}(urea)_2(H_2O)]_2[Nb^{IV}(CN)_8]\}_n$ revealing significant MSHG (magnetization-induced second harmonic generation).[25] In search of porous hybrid networks, the new pathway leading to extended structures through organization of high-spin $M^{II}_9[W^{V}(CN)_8]_6$ (M = Mn, Co, Ni) clusters by organic bridging ligands was explored.[26]

Here we present a complete and up-to-date overview of octacyanometallate-based structures obtained in the first decade of the 21st century. The detailed classification of known topologies unveils general rules governing the self-assembly processes. The variety of functionalities is demonstrated on the basis of most appealing examples chosen from the abundance of characterized compounds. The perspectives of further development and potential applications are outlined in the final section.

2. Topology and Structural Patterns

The structures of octacyanometallate-based coordination networks is described by using popular topological terminology (3,2 chains, square grids, honeycombs etc.),[27] as well as by the generalized notation adapted from Cheetham and co-workers I^nO^n, where I^n denotes inorganic connectivity and O^n denotes organic connectivity, n = 0, 1, 2 or 3.[28] According to this notation, octacyanide-based assemblies can be shortly classified into three general groups: *discrete molecular species* (I^0O^0) with local inorganic and/or organic bridging, *inorganic networks* (I^nO^0) with extended inorganic connectivity only and *hybrid organic–inorganic networks* (I^nO^n). The second group comprises purely inorganic cyanide-bridged networks as well as cyanide-bridged networks with organic constituents acting only as blocking ligands or counterions. The third group relates to the recently reported assemblies and may be further divided into: *extended inorganic hybrids* (I^nO^0) with extended inorganic connectivity and local organic bridging, *coordination polymers* (I^0O^n) with extended organic connectivity and discrete inorganic clusters and *mixed organic–inorganic hybrids* (I^nO^n, $n > 0$ in both cases) with combined inorganic and organic connectivity, each at least in one dimension.

It is worth noting that, according to the original Cheetham notation, the sum of the dimensionalities of inorganic and organic connectivity ($n + n$) gives the overall dimensionality of the framework. Thus, the networks denoted as I^3O^0, I^2O^1, I^1O^2 and I^0O^3 stand for the limiting point for mixed topological patterns. However, in recent years it was shown that combining octacyanometallates with d and f metal centres and polytopic organic ligands may lead to the novel types of networks denoted as I^3O^1 or I^2O^2, inorganic M′–CN–M and metal–organic M′–L–M′ subnetworks cross-linking at metallic centres.

2.1. Inorganic Networks

2.1.1. 0D Assemblies

Molecular bimetallic and trinuclear discrete assemblies based on octacyanometallates comprise a large variety of compounds.[13–15,29–72] They range from dinuclear species through pentadecanuclear clusters to the largest characterized eicosanuclear cluster (Table 1). The most characteristic shapes of clusters are presented in Figure 3.

The discrete compounds can be roughly divided into three groups: those containing (1) one, (2) two or (3) more octacyanometallate units. The first group comprises dimers, trimers with linear or angular shape and star-shaped molecules incorporating up to six cationic complexes.[29–49] The star-like clusters are achieved when a polydentate blocking ligand leaves only one coordination site for cyanide bridging and were so far obtained only with octacyanomolybdate (IV) as a centre. Among the clusters comprising two octacyanometallate ions, the most common are squares,[42,52–59] but trigonal[60] and tetragonal bipyramids[13,59,61,62] are also observed (Figure 3a, b). They are usually formed when an octahedral cationic complex includes two bidentate ligands like bpy or phen and has two *cis* positions available for bridging. It is worth noting that tetragonal bipyramid clusters are unique to octacyanometallates, as they employ the

Table 1. Discrete molecules (I^0O^0).[a]

Molecular formula	Cluster core	Topological pattern	Ref.
$[Ni^{II}(en)_3][Ni^{II}(en)_2(H_2O)W^{IV}(CN)_8]$	NiW	dimer	[29]
$[Mn^{III}(L^1)(H_2O)_2]_2[\{Mn^{III}(L^1)(H_2O)\}\{W(CN)_8\}_2]\cdot 2H_2O$	MnW		[30]
$[M^{II}(en)_3][\{M^{II}(en)_2(H_2O)][M^{IV}(CN)_8]\}\cdot 2H_2O$ (M^{II} = Mn, Ni; M^{IV} = Mo, W)	$M^{II}M^{IV}$		[31]
$[Ln(terpy)(dmf)_2(H_2O)_2][W(CN)_8]\cdot 3H_2O$ (Ln = Ho, Er, Yb)	LnW		[32]
$Cs^I_2[Pt^{II}(en)_2Cl_2]\{[Pt^{IV}(en)_2][Mo^{IV}(CN)_8]_2\}\cdot 10H_2O$	$PtMo_2$	linear trimer	[33]
$[Ni(L^2)(H_2O)_2]_2\{[Ni(L^2)][M^V(CN)_8]_2\}$ (M = Mo, W)	NiM_2		[34]
$\{[Cu^{II}(tn)_2]_2[Mo^{IV}(CN)_8]\}\cdot 2H_2O$	Cu_2Mo		[35]
$\{[Cu^{II}(L^3)]_2[Mo^{IV}(CN)_8]\}\cdot 6H_2O$	Cu_2Mo	V-shaped trimer	[36]
$\{[Cu^{II}(bpy)_2]_2[Mo^{IV}(CN)_8]\}\cdot CH_3OH\cdot 5H_2O$	Cu_2Mo		[37,38]
$[Mn^{III}(L^4)(H_2O)_2]\{[Mn^{III}(L^4)(H_2O)]_2[W^V(CN)_8]\}$	Mn_2W		[39]
$\{[Ni(L^2)(H_2O)]_2[M^V(CN)_8]\}$ (M = Mo, W)	Ni_2M		[34]
$\{[Ni^{II}(en)_2(H_2O)]_2[Mo^{IV}(CN)_8]\}\cdot 2H_2O$	Ni_2Mo		[40]
$\{[M^{II}(en)_2(H_2O)]_2[M^{IV}(CN)_8]\}\cdot 4H_2O$ (M^{II} = Co, M^{IV} = Mo, W; +Ni,Mo)	$M^{II}_2M^{IV}$		[31]
$[\{L^5Ni(dmf)Ln(dmf)_4\}\{W(CN)_8\}]\cdot H_2O$ (Ln = Gd, Dy)	NiLnW		[41]
$[\{L^5Ni(dmf)Tb(dmf)_4\}\{W(CN)_8\}]\cdot 0.5dmf$	NiTbW		[41]
$[\{L^5Ni(dmf)Ho(dmf)_4\}\{W(CN)_8\}]\cdot 2H_2O$	NiHoW		[41]
$[\{L^5Ni(dmf)Gd(dmf)_3(H_2O)\}\{W(CN)_8\}]\cdot H_2O\cdot 0.5thf\cdot 0.5dmf$	NiGdW		[41]
$[\{L^5Ni(H_2O)Tb(dmf)_{2.5}(H_2O)_{1.5}\}\{W(CN)_8\}]\cdot H_2O\cdot 0.5dmf$	NiTbW		[41]
$[\{L^5Ni(H_2O)Er(dmf)_3(H_2O)\}\{W(CN)_8\}]\cdot H_2O\cdot 0.5dmf$	NiErW		[41]
$\{[Cu(bpy)_2]_2[W^V(CN)_8]\}\{[Cu(bpy)_2][W^V(CN)_8]\}\cdot 4H_2O$	Cu_2W+CuW	trimer + dimer	[42]
$\{[Cu(L^6)]_2[W(CN)_8]\}\{[Cu(L^6)][W(CN)_8]\}$	Cu_2W+CuW		[43]
$\{[Mn^{III}(salen)(H_2O)]_3[W^V(CN)_8]\}\cdot H_2O$	Mn_3W	V-shaped molecule	[44]
$[Ce_2(bpm)(dmso)_8(H_2O)_4][W(CN)_8]_2\cdot 4H_2O$	Ce_2W_2		[45]
$\{[Mn^{II}(bpy)_2][Mn^{II}(bpy)_2(H_2O)]_2[W^V(CN)_8]_2\}\cdot 7H_2O$	Mn_3W_2		[46]
$[\{L^5NiLa(H_2O)_{4.5}\}_2\{W(CN)_8\}_2]\cdot 9H_2O$	$Ni_2La_2W_2$		[47]
$[\{L^5Ni(H_2O)Ln(H_2O)_{4.5}\}_2\{W(CN)_8\}_2]\cdot 15H_2O$ (Ln = Gd, Tb, Dy)	$Ni_2Ln_2W_2$		[48]
$\{[Ni^{II}L^7]_3[Mo^{IV}(CN)_8]\}(ClO_4)_2\cdot 4H_2O$	Ni_3Mo	star-like molecule	[49]
$\{[Cu^{II}(L^8)]_2[Cu^{II}(L^8)(H_2O)]_2[Mo^{IV}(CN)_8]\}\cdot 6H_2O$	Cu_4Mo		[50]
$\{[Cu^{II}(L^9)]_3[Cu^{II}(L^9)(H_2O)]_2[Mo^{IV}(CN)_8]\}\cdot 10H_2O$	Cu_8Mo_2		[50]
$\{[Cu^{II}(tren)]_6[Mo^{IV}(CN)_8]\}(ClO_4)_8$	Cu_6Mo		[51]
$\{[Ni^{II}L^7]_6[Mo^{IV}(CN)_8]\}(ClO_4)_8\cdot 10H_2O$	Ni_6Mo		[49]
$[Cu^{II}(phen)_3]_2\{[Cu^{II}(phen)_2]_2[W(CN)_8]_2\}(ClO_4)_2\cdot 10H_2O$	Cu_2W_2	square	[42]
$\{[Ni^{II}(HL^{10})]_2[W^V(CN)_8]_2\}$	Ni_2W_2		[52]
$\{[Mn^{II}(bpy)_2]_2(oxalate)\}\{[Mn^{II}(bpy)_2]_2[W^V(CN)_8]_2\}\cdot 4H_2O$	Mn_2W_2		[53]
$[Mn^{II}(tptz)(CH_3COO)(H_2O)_2]_2[Mn^{II}(tptz)(CH_3OH)_{1.58}(H_2O)_{0.48}]_2$ $[W^V(CN)_8]_2\cdot 5CH_3OH\cdot 9.85H_2O$	Mn_2W_2		[54]
$[M^{II}(tpm)_2][W^V_2(CN)_{16}M^{II}_2(tpm)_2(H_2O)_2]\cdot 4H_2O$ (M = Co, Mn)	M_2W_2		[55]
$[Mn^{II}(phen)_3]_2[Mn^{II}(phen)_2(\mu\text{-}NC)_2W^V(CN)_6]_2(ClO_4)_2\cdot 9H_2O$	Mn_2W_2		[56]
$K_2\{[Co^{II}(tren)]_2[W^{IV}(CN)_8]_2\}\cdot 9H_2O$	Co_2W_2		[57]
$\{[Mn^{II}(tptz)(CH_3OH)(NO_3)]_2[Mn^{II}(tptz)(CH_3OH)(dmf)]_2[W^V(CN)_8]_2\}\cdot 6CH_3OH$	Mn_4W_2	decorated square	[54]
$[(Mo(CN)_8)_2(CuL^{11}Tb)_4](Mo(CN)_8)$		decorated square	[58]
$\{[Mn^{II}_6(tptz)_6(CH_3OH)_4(dmf)_2]_2[W^V(CN)_8]_4\}\cdot 2.3CH_3OH\cdot 8.2H_2O$	Mn_6W_4	tripled squared	[54]
$\{[Mn(phen)_2(H_2O)]_2[Mn(phen)_2]_4[M^{IV}(CN)_8]_3\}\cdot 21H_2O$ (M = Nb, W)	Mn_6M_3	decorated doubled square	[59]
$[Ni^{II}(tmphen)_2]_3[M^V(CN)_8]_2$ (M = Mo, W)	Ni_3M_2	trigonal bipyramid	[60]
$\{[Mn^{II}(bpy)_2]_4[Nb^{IV}(CN)_8]_2\}$	Mn_4Nb_2	octahedron	[59]
$\{[Mn^{II}(bpy)_2]_4[M^{IV}(CN)_8]_2\}\cdot nH_2O$ (M = Mo, W; n = 14, 9)	Mn_4M_2 (M = Mo, W)		[13,21,61]
$\{[Co(phen)_2]_4[CoCl(phen)_2]_2[W(CN)_8]_2\}$	Co_6W_2	decorated octahedron	[62]
$\{[Mn^{II}[Mn^{II}(CH_3OH)_3]_8][Re^V(CN)_8]_6\}\cdot CH_3OH\cdot 7.8H_2O$	Mn_9W_6	six-capped body-centred cube	[63]
$\{[Mn^{II}[Mn^{II}(CH_3CH_2OH)_3]_8][Mo^V(CN)_8]_6\}\cdot 6CH_3CH_2OH\cdot 3(CH_3)_2CHOH\cdot 3H_2O$	Mn_9W_6		[64]
$\{[Mn^{II}[Mn^{II}(CH_3CH_2OH)_3]_8][W^V(CN)_8]_6\}\cdot 12CH_3CH_2OH$	Mn_9W_6		[14]
$\{[Mn^{II}[Mn^{II}(CH_3OH)_3]_8][Mo^V(CN)_8]_6\}\cdot 5CH_3OH\cdot 2H_2O$	Mn_9W_6		[15]
$\{[Ni^{II}[Ni^{II}(CH_3OH)_3]_8][Mo^V(CN)_8]_6\}\cdot 17CH_3OH\cdot H_2O$	Ni_9Mo_6		[65]
$\{[Ni^{II}[Ni^{II}(CH_3OH)_3]_8][W^V(CN)_8]_6\}\cdot 15CH_3OH$	Ni_9W_6		[65]
$\{Ni^{II}[Ni^{II}(tmphen)(CH_3OH)]_6[Ni(H_2O)_3]_2[M^V(CN)_8]_6\}$ (M = Mo, W)	Ni_9M_6		[60]
$\{Ni^{II}[Ni^{II}(btz)(CH_3OH)]_8[W^V(CN)_8]_6\}\cdot 18H_2O\cdot 6CH_3OH$	Ni_9W_6		[66]
$\{Ni^{II}[Ni^{II}(bpy)(H_2O)]_8[W^V(CN)_8]_6\}\cdot 41H_2O$	Ni_9W_6		[67]
$\{Ni^{II}[Ni^{II}(bpy)(H_2O)]_8[Mo^V(CN)_8]_6\}\cdot 12H_2O$	Ni_9Mo_6		[68]
$\{Co^{II}[Co^{II}(CH_3OH)_3]_8[M^V(CN)_8]_6\}\cdot nH_2O\cdot mCH_3OH$ (M^V = Mo, W)	Co_9W_6		[69]
$[\{Cu_3(L^{12})(OH_2)\}_2\{Mo(CN)_8\}](NO_3)_8\cdot 15H_2O$	Cu_6Mo	spherical molecule	[70]
$[\{NiL^{13}\}_{12}\{Nb(CN)_8\}_6]$	$Ni_{12}Nb_6$	decorated 12-metallic ring	[71]
$[Cu(H_2O)\{Cu(Me_3tacn)\}_{12}\{W^V(CN)_8\}_2\{W^{IV}(CN)_8\}_5]\cdot 24H_2O$	$Cu_{13}W_7$	20-metallic open-winged cage	[72]

[a] bpm = 2,2′-bipyrimidine; bpy = 2,2′-bipyridine; btz = 2,2′-bi(4,5-dihydrothiazine); dmf = *N*,*N*-dimethylformamide; dmso = dimethyl sulfoxide; en = ethylenediamine; L^1 = *N*,*N*′-phenylenebis(3-methoxysalicylideneiminato) dianion; L^2 = {2,12-dimethyl-3,7,11,17-tetrazabicyclo[11.3.1]heptadeca-1(17),2,11,13,15-pentaene}; L^3 = 1,4-bis(3-aminopropyl)piperazine; L^4 = *N*,*N*′-(1-methylethylene)bis(5-chlorosalicylideneiminato) dianion; L^5 = *N*,*N*′-2,2-dimethylpropylenebis(3-methoxysalicylideneiminato) dianion; L^6 = 3,7-bis(2-aminoethyl)-1,3,5,7-tetraazabicyclo[3.3.2]decane; L^7 = 2-[6-(2-amino-1-aminomethyl-1-methyl-ethyl)pyridin-2-yl]-2-methylpropan-1,3-diamine; L^8 = *N*-[(2-pyridyl)methyl]salicyliminato ion; L^9 = *N*-[(2-pyridyl)ethyl]salicyliminato ion; L^{10} = 7-(3-ammoniopropyl)-2,12-(pyridine-2,6-diyl)-3,7,11-triazatrideca-2,11-diene; L^{11} = *N*,*N*′-bis(3-methoxysalicylidene)ethylenediamine; L^{12} = 1,3,5-triazine-2,4,6-triyltris[3-(1,3,5,8,12-pentaazacyclotetradecane)]; L^{13} = 2,12-dimethyl-3,7,11,17-tetraazabicyclo[12.3.1]heptadeca-1(17),2,11,12,15-pentadiene; Me_3tacn = 1,4,7-trimethyl-1,4,7-triazacyclononane; phen = 1,10-phenanthroline; salen = *N*,*N*′-ethylenebis(salicylideneiminato) dianion; terpy = 2,2′:6′,2″-terpyridine; thf = tetrahydrofuran; tmphen = 3,4,7,8-tetramethyl-1,10-phenanthroline; tn = 1,3-diaminopropane; tpm = tri(1*H*-pyrazol-1-yl)methane; tptz = 2,4,6-tris(2-pyridyl)-1,3,5-triazine; tren = tris(2-aminoethyl)amine.

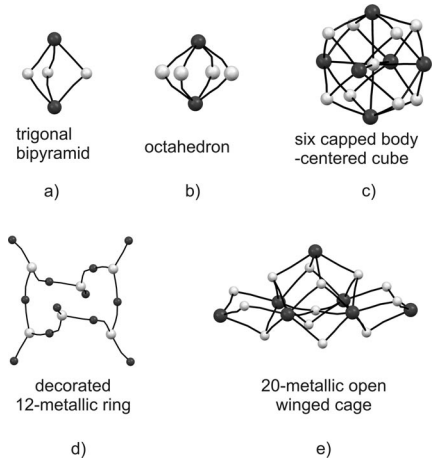

Figure 3. The most important types of coordination skeletons in octacyanometallate-based clusters (a–c) and the skeletons of the biggest clusters: $Ni_{12}Nb_6$ decorated ring (d) and W_7Cu_{13} winged cage (e). Dark grey spheres: Mo, W or Nb; light grey spheres: 3d metals; black sticks: CN^- bridges. Blocking and terminal ligands are omitted for clarity.

square antiprism geometry of the anion, and cannot be formed by octahedral hexacyanometallates. Within the higher nuclearity clusters a small class of square-based oligomeric chain-like species can be observed.[54,59] However, the most characteristic for octacyanometallates is the cubane-shaped pentadecanuclear cluster[14,15,60,63–69] (Figure 3c) obtained in alcohol or mixed water/alcohol media. Its central cation is surrounded by six octacyanometallates forming an octahedron, and each of the octacyanometallates forms additional four bridges to the remaining cations placed at the corners of a cube. Such clusters are readily formed by octahedral bivalent cations Co, Mn and Ni if three facial coordination sites are available. Interestingly, even if the remaining three ligands are weakly coordinating, the reaction does not proceed spontaneously to extended structures. The second largest discrete assembly is the octadecanuclear system $Ni^{II}{}_{12}Nb^{IV}{}_6$ built of the Nb_6Ni_6 cyclic skeleton with six additional Ni units dangling at Nb sites, obtained by using Ni complexes blocked equatorially with a cyclic ligand (Figure 3d).[71] This oligomer can be considered a cyclic form related to the open-chain structure observed in other compounds with analogous cationic complexes. The largest $Cu_{13}W_7$ cluster was obtained from Cu^{II} with tridentate *fac*-blocking ligand (Figure 2e).[72] In this case, a pentadecanuclear cluster was not formed because of O_h symmetry breaking by the Jahn–Teller effect. The central Cu atom forms four equatorial cyanide bridges and axially binds one water molecule to give a tetragonal pyramidal environment. The cluster additionally comprises twelve hexa- or pentacoordinate Cu atoms and seven octacyanotungstates arranged in the twofold symmetry of a winged-opening cage.

The separate class of compounds are the trimetallic molecules based on bimetallic dinuclear $\{(M^{II}L)_2Ln^{III}\}$ species bridged by $[M^V(CN)_8]^{3-}$. By analogy to the bimetallic species, cyanide bridging may lead to trinuclear and hexanuclear open-chain or decanuclear closed-ring oligomers.[41,47,48]

2.1.2. 1D Assemblies

The overview of topologies of 1D systems based on octacyanometallates is shown in Table 2.[32,44,54,71,73–94] All of the presented structural patterns can be divided in two main groups. The first group, consisting of chains built on single cyanide bridges only, is shown in Figure 4a–c.[32,44,54,71,73–82] The T-shaped chains are generally observed in systems built of complexes with polyamine ligands, while more bulky and rigid Schiff bases of open or closed structure may lead to the helical chain with pendant arms. The interesting structural motif of two different types of chains can be seen in the $\{[Mn^{II}_2(tptz)_2(MeOH)_3W^V(CN)_8][Mn^{II}(tptz)(MeOH)W^V(CN)_8]\cdot 2H_2O\cdot MeOH\}_\infty$ system.[54] Generally, decorated chains are observed for structures with divalent 3d cations, while simple bimetallic chains are formed in the case of trivalent Ln^{III} cations.

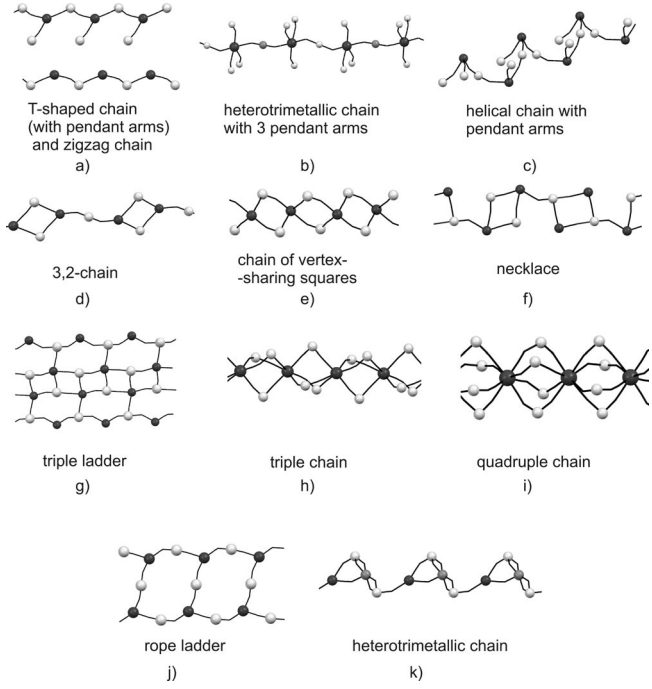

Figure 4. Topological and structural patterns in 1D systems. Dark grey spheres: Mo, W or Nb; light grey spheres: 3d metals; black sticks: CN^- bridges. Blocking and terminal ligands are omitted for clarity.

The second group of 1D topologies contains polynuclear rings.[54,83–94] Typically, the rings in 1D systems contain four metal centres. One of the most frequently observed structural motifs is 3,2-chain (Figure 4d) found in compounds based on $[W^V(CN)_8]^{3-}$ ions and M^{2+} complexes with neutral ligands, which can be attributed to the charges of the building blocks and the metal ratio. On the other hand, in systems containing $[W^{IV}(CN)_8]^{4-}$ units, the ratio changes to 2:1, and a chain of vertex sharing squares topology is formed (Figure 4e). In the case of 1:1 metal centres, the

Table 2. 1D inorganic networks (I^1O^0).[a]

Molecular formula	Topological pattern	Ref.
$[Mn^{II}_2(L^{14})_2(H_2O)][Mo^{IV}(CN)_8]\cdot 5H_2O$	chiral helical chain with pendant arms	[73]
$[\{Mn^{II}(L^{14})\}_2\{Nb^{IV}(CN)_8\}(H_2O)]_\infty$		[71]
$[\{(H_2O)Fe(L^{14})\}\{M^{IV}(CN)_8\}\{Fe(L^{14})\}]_\infty$ (M = Nb, Mo, W)		[74]
$[Mn^{III}(5\text{-Clsalen})(H_2O)(CH_3OH)][Mn^{III}(5\text{-Clsalen})(H_2O)][Mn^{III}(5\text{-Clsalen})Mo(CN)_8]\cdot 3H_2O$		[75]
$[Mn^{III}(5\text{-Brsalen})(H_2O)_2][Mn^{III}(5\text{-Brsalen})(H_2O)][Mn^{III}(5\text{-Brsalen})W(CN)_8]\cdot H_2O\cdot 3CH_3OH$		[75]
$\{[Mn^{II}_2(tptz)_2(CH_3OH)_3(CH_3COO)][W^{V}(CN)_8]\cdot 3.5CH_3OH\cdot 0.25H_2O\}_\infty$		[54]
$[Mn(salen)(H_2O)_2]_2[Mn(salen)(H_2O)][Mn(salen)]_2[Mo(CN)_8]\cdot 0.5ClO_4\cdot 0.5OH\cdot 4.5H_2O$	zigzag chain	[44]
$[Nd(pzam)_3(H_2O)Mo(CN)_8]\cdot H_2O$		[76]
$[Gd(pzam)_3(H_2O)M(CN)_8]\cdot H_2O$ (M = Mo, W)		[77]
$[Tb(pzam)_3(H_2O)Mo(CN)_8]\cdot H_2O$		[78]
$Gd^{III}(dma)_n[W^{V}(CN)_8]$ (n = 5,6)		[79]
$[Ln(terpy)(dmf)_4][W(CN)_8]\cdot 6H_2O\cdot CH_3CH_2OH$ (Ln = Ce,Pr,Nd,Sm,Eu,Gd,Tb,Dy)		[32,80,81]
$\{[trans\text{-}Ni^{II}(tn)_2(OH_2)][trans\text{-}Ni^{II}(\mu\text{-}NC)_2(tn)_2][(\mu\text{-}NC)_3M^{IV}(CN)_5]\cdot 6H_2O\}$ (M^{IV} = Mo, W)	T-shaped chain	[82]
$\{[Mn^{II}_2(tptz)_2(CH_3OH)_3W^{V}(CN)_8]$ $[Mn^{II}(tptz)(CH_3OH)W^{V}(CN)_8]\cdot 2H_2O\cdot CH_3OH\}_\infty$	T-shaped chain with pendant arms + zigzag chain	[54]
$\{[Mn^{II}(tptz)(CH_3OH)]_2[W^{IV}(CN)_8]\cdot 2CH_3OH\}_\infty$	chain of vertex-sharing squares	[54]
$\{[Mn^{II}(bpy)(dmf)_2]_2[Mo^{IV}(CN)_8]\cdot 1.5H_2O\}_n$		[83]
$[Ni^{II}(tren)]_3[Mo^{IV}(CN)_8](ClO_4)_2\cdot 5H_2O$	chiral triple-chain	[84]
$\{[W^{V}(CN)_8][Cu^{II}(dien)_4]_3[W^{V}(CN)_8]^{5+}\}_\infty$	quadruple chain	[85]
$[Cu^{II}(tetrenH_2)]_2[W^{IV}(CN)_8]_2\cdot 5H_2O$	necklace	[86]
$\{[Mn(bpy)_2(dmf)_2]_2[Mo^{V}(CN)_8]_2[Mn(dmf)_4]\}_\infty$	3,2-chain	[87]
$\{[Co^{II}_3(dmf)_{12}][W^{V}(CN)_8]_2\}_\infty$		[88]
$\{[Mn^{II}_3(bpy)_2(dmf)_8][W^{V}(CN)_8]_2\}_\infty$		[88]
$\{[trans\text{-}Mn^{II}(dmf)_4][cis\text{-}Mn^{II}(dmf)_4]_2[W^{V}(CN)_8]_2\}_n$		[89]
$\{[trans\text{-}Ni^{II}(dmf)_4][cis\text{-}Ni^{II}(dmf)_4]_2[W^{V}(CN)_8]_2\}_n$		[89]
$[Cu^{II}(tetrenH_2)][Cu^{II}(tetrenH)][W^{V}(CN)_8][W^{IV}(CN)_8]\cdot 2.5H_2O$	triple ladder	[86]
$[Cu^{II}(cyclam)]_3[W^{V}(CN)_8]_2\cdot 5H_2O$	rope-ladder	[90]
$[Cu^{II}(cyclam)]_3[Mo^{V}(CN)_8]_2\cdot 5H_2O$		[91]
$\{Cs[Sm(CH_3OH)_3(dmf)(H_2O)Mo(CN)_8]\cdot H_2O\}_n$		[92]
$[(Ni^{II}(cyclam))(Mo^{IV}(CN)_8)_2(Cu^{II}(me_2en)_2)_7](ClO_4)_8$	heterotrimetallic chain with 3 pendant arms	[93]
$[\{(CuL^{15})_2Gd\}\{Mo(CN)_8\}]\cdot 2CH_3CN$	heterotrimetallic chain	[94]
$[\{(CuL^{15})_2Dy\}\{Mo(CN)_8\}]\cdot CH_3CN\cdot H_2O$		[94]
$[\{(CuL^{15})_2La\}\{W(CN)_8\}]\cdot 2H_2O$		[94]
$[\{(CuL^{15})_2Gd\}\{W(CN)_8\}]\cdot 2CH_3CN$		[94]
$[\{(CuL^{15})_2Dy\}\{W(CN)_8\}]\cdot 4CH_3CN$		[94]

[a] 5-Brsalen = *N*,*N*′-ethylenebis(5-bromosalicylideneiminato) dianion; 5-Clsalen = *N*,*N*′-ethylenebis(5-chlorosalicylideneiminato) dianion; bpy = 2,2′-bipyridine; cyclam = 1,4,8,11-tetraazacyclotetradecane; dien = diethylenetriamine; dma = dimethylacetamide; dmf = *N*,*N*-dimethylformamide; L^{14} = 2,13-dimethyl-3,6,9,12,18-pentaazabicyclo-[12.3.1]octadeca-1(18),2,12,14,16-pentaene; L^{15} = *N*,*N*′-propylenebis(3-methoxysalicylideneiminato) dianion; me_2en = *N*,*N*-dimethylethylenediamine; pzam = pyrazine-2-carboxamide; terpy = 2,2′:6′,2′′-terpyridine; tetren = tetraethylenepentaamine; tn = 1,3-diaminopropane; tptz = 2,4,6-tris(2-pyridyl)-1,3,5-triazine; tren = tris(2-aminoethyl)amine.

ratio observed in two of our systems $[Cu^{II}(tetrenH_2)]_2[W^{IV}(CN)_8]_2\cdot 5H_2O$ and $[Cu^{II}(tetrenH_2)][Cu^{II}(tetrenH)][W^{V}(CN)_8][W^{IV}(CN)_8]\cdot 2.5H_2O$ exploiting 5- and 6-coordination in Cu^{II} complexes with partially protonated forms of the tetren ligand, the cyanide-bridged skeletons reveal the original topologies of necklace and triple ladder (Figure 4f, g), respectively.[86] The increasing ratio of $ML^{n+}/[M(CN)_8]^{m-}$ together with polyamine chelating L ligands leads to the formation of a triple chain topology (L = tren, M = Mo^{IV})[84] and a quadruple chain (L = dien, M = W^{V})[85] with the highest possible number of cyanide bridges within the chain based on $[M(CN)_8]^{n-}$ ions (Figure 4h, i). The enhanced connectivity between metal centres leads to the formation of the rope-ladder pattern in the case of assemblies based on octacyanometallate(V) and copper complexes of cyclam (Figure 4j).[90,91] Due to the sterically demanding $[Cu(cyclam)]^{2+}$ units, the rings are formed with eight metallic centres. The original coordination skeleton was obtained by Sutter at al. for $[\{(CuL^{15})_2Ln\}\{Mo(CN)_8\}]\cdot 2CH_3CN$, in which Mo is bridged by two CN^- ligands to Cu^{II} and to the Ln^{III} centre in the same $\{(CuL^2)_2Ln\}$ dimer (Figure 4k).[94]

2.1.3. 2D Assemblies

The 2D polymeric skeletons are collected in Table 3 and reveal the topologies of honeycomb, brick-wall and square grid presented in Figure 5a–d.[18a,18b,19d,24,89,90–114] The honeycomb motif in $\{[Ni^{II}(cyclam)]_3[W^{V}(CN)_8]_2\}_n$ and

$[Cu^{II}(L)]_3[M^V(CN)_8]_2 \cdot n$solv (L = substituted tetraazamacrocyclic ligands; M = Mo, W)[24,90] is preferred as a result of the presence of bulky macrocyclic ligands. The systems containing smaller terminal ligands, such as *N*,*N*′-dimethylformamide, display brick-wall-type structures.[89,98] In these two topological patterns, 12-metallic rings are typically observed. The square-grid networks consist typically of 4-metallic rings with both types of centres as nodes and are generally realized in $\{Ln(H_2O)_5[M(CN)_8]\}$ (Ln = lanthanide) networks[102–105] and $\{M(3\text{-}CNpy)_2[M(CN)_8]\}$ (M = Mn, Co) networks[99,106] with a 1:1 stoichiometry of metallic centres. We have shown that these structural motifs could be obtained in more extended form with Cu^{II} complexes. A unique square grid with pendant arms is present in $[Cu^{II}(tren)][Cu^I\{W^V(CN)_8\}] \cdot 1.5H_2O$ with two different oxidation states of copper (Figure 5e).[113] In the presence of fully protonated polyamine ligands, the family of double-layered systems $\{(dienH_3)Cu^{II}_3[M^V(CN)_8]_3 \cdot 4H_2O\}_n$ and $\{(tetrenH_5)_{0.8}Cu^{II}_4[M^V(CN)_8]_4 \cdot 7.2H_2O\}_n$ (M = Mo, W) is formed (Figure 5f).[18,19d] In this case, the absence of the sixfold coordinated site at Cu prevents the molecular structure from developing into a 3D network. Extended square-grid networks consisting of 8-metallic rings, in which $[M(CN)_8]^{n-}$ stand for nodes and 3d metals are located on the edges of the ring, were observed for $[Cu^{II}(dien)]_2[M^{IV}(CN)_8] \cdot 4H_2O$ (M = Mo, W) (Figure 5d)[86,100] or $[\{Cu(3\text{-}CNpy)_2(H_2O)\}_2\{Cu(3\text{-}CNpy)_2(H_2O)_2\}\{W(CN)_8\}_2]$ (Figure 5g) and other compounds.[110,112]

Table 3. 2D inorganic networks (I^2O^0).[a]

Molecular formula	Topological pattern	Ref.
$[Cu(L^{16})]_3[Mo(CN)_8]_2 \cdot 10H_2O \cdot 2CH_3CN$	honeycomb	[90]
$[Cu(L^{16})]_3[W(CN)_8]_2 \cdot 10H_2O \cdot 2CH_3CN$		[90]
$[Cu(L^{17})]_3[W(CN)_8]_2 \cdot 2H_2O$		[90]
$\{[Ni^{II}(cyclam)]_3[W^V(CN)_8]_2\}_n$		[24]
$[Cu^{II}(L^{18})]_3[Mo^V(CN)_8]_2 \cdot 6H_2O \cdot 2CH_3OH$		[95]
$[Cu^{II}(L^{18})]_3[W^V(CN)_8]_2 \cdot 6H_2O \cdot 2CH_3OH$		[95]
$[Cu^{II}(L^{19})]_3[Mo^V(CN)_8]_2 \cdot 6H_2O$		[96]
$[Cu^{II}(L^{19})]_3[W^V(CN)_8]_2 \cdot 6H_2O$		[96]
$\{[Cu^{II}(L^{20})]_3[W^V(CN)_8]_2\} \cdot [Cu^{II}(L^{20}) \cdot 2H_2O] \cdot (ClO_4)_2 \cdot 4H_2O$	brick wall	[97]
$\{[trans\text{-}Ni^{II}(dmf)_4][cis\text{-}Ni^{II}(dmf)_4]_2[W^V(CN)_8]_2\}_n$		[89]
$\{[trans\text{-}Fe^{II}(dmf)_4][cis\text{-}Fe^{II}(dmf)_4]_2[W^V(CN)_8]_2\}_n$		[89]
$\{[Mn^{II}(dmf)_4]_3[Mo^V(CN)_8]_2\}_n$		[98]
$[Cu^{II}(L^{21})]_2[Mo^{IV}(CN)_8] \cdot 6.75H_2O$	square grid	[83]
$Cs^I[\{Co^{II}(3\text{-}CNpy)_2\}\{W^V(CN)_8\}] \cdot H_2O$		[99]
$[Cu^{II}(dien)]_2[M^{IV}(CN)_8] \cdot 4H_2O$ (M = Mo, W)		[86]
$[Cu(tn)_2]_2[W(CN)_8](OH) \cdot H_2O$		[100]
$\{[Cu(dien)]_2[W(CN)_8](OH) \cdot 3H_2O\}_\infty$		[100]
$Sm(H_2O)_5[W(CN)_8]$		[101]
$Ln(H_2O)_5[M(CN)_8]$ (Ln = Eu, Gd, Tb; M = Mo, W)		[102,103]
$\{Sm(H_2O)_9[Sm_2(bpy)_2(H_2O)_2(OH)_{2.75}(NO_3)_{0.25}][Mo(CN)_8]_2\}_n$		[104]
$Ln(H_2O)_5[W(CN)_8]$ (Ln = La, Pr, Nd, Eu, Gd)		[105]
$Ln(H_2O)_4[W(CN)_8]$ (Ln = Ho, Er, Tm, Lu)		[105]
$Cs^I[Mn^{II}(3\text{-}CNpy)_2\{W^V(CN)_8\}] \cdot H_2O$		[106]
$[Cu(cyclam)]_2[Mo(CN)_8] \cdot 10.5H_2O$		[107,108]
$[Mo(CN)_8Ni_2(pn)_4]_n \cdot 4nH_2O$	folded square grid with 8 and 4 metallic units	[109]
$[Cu(tn)]_3[W(CN)_8]_2 \cdot 3H_2O$		[110]
$[Cu(pn)]_3[W(CN)_8]_2 \cdot 3H_2O$		[110]
$[W(CN)_8]_4[Cu\{(S)\text{-}pn\}H_2O]_4[Cu\{(S)\text{-}pn\}]_2 \cdot 2.5H_2O$		[111]
$[W(CN)_8]_4[Cu\{(R)\text{-}pn\}H_2O]_4[Cu\{(R)\text{-}pn\}]_2 \cdot 2.5H_2O$		
$[W(CN)_8]_4[Cu\{(rac)\text{-}pn\}H_2O]_4[Cu\{(rac)\text{-}pn\}]_2 \cdot 2.5H_2O$		
$[\{Cu(3\text{-}CNpy)_2(H_2O)\}_2\{Cu(3\text{-}CNpy)_2(H_2O)_2\}\{W(CN)_8\}_2]$		[112]
$[\{Cu(4\text{-}CNpy)_2\}_2\{Cu(4\text{-}CNpy)_2(H_2O)_2\}\{W(CN)_8\}_2] \cdot 6H_2O$		[112]
$[Cu^{II}(tren)]\{Cu^I[W^V(CN)_8]\} \cdot 1.5H_2O$	square grid with pendant arms	[113]
$Cs^ICu^{II}[W^V(CN)_8] \cdot 0.5H_2O$	bilayered square grid	[19e]
$\{(tetrenH_2)_{0.5}[Mn(H_2O)_2][Mo^V(CN)_8] \cdot 2H_2O\}_n$	bilayered square grid (4-metallic rings)	[114]
$\{(tetrenH_5)_{0.8}Cu^{II}_4[W^V(CN)_8]_4 \cdot 7.2H_2O\}_n$	bilayered square grid	[18a]
$\{(tetrenH_5)_{0.8}Cu^{II}_4[Mo^V(CN)_8]_4 \cdot 7.2H_2O\}_n$	bilayered square grid	[18b]
$\{(dienH_3)Cu^{II}_3[W^V(CN)_8]_3 \cdot 4H_2O\}_n$	bilayered square grid	[18b]
$\{(dienH_3)Cu^{II}_3[Mo^V(CN)_8]_3 \cdot 4H_2O\}_n$	bilayered square grid	[18b]

[a] 3-CNpy = 3-cyanopyridine; 4-CNpy = 4-cyanopyridine; bpy = 2,2′-bipyridine; cyclam = 1,4,8,11-tetraazacyclotetradecane; dien = diethylenetriamine; dmf = *N*,*N*-dimethylformamide; L^{16} = 6,13-bis(3-hydroxypropyl)-1,4,6,8,11,13-hexaazacyclotetradecane; L^{17} = 5,12-dimethyl-2,3:9,10-bis(tetramethylene)-1,4,8,11-tetraazatetradecane; L^{18} = 3,14-diethyl-2,6,13,17-tetraazatricyclo(16.4.0.07,12)docosane; L^{19} = 3,10-bis(2-hydroxypropyl)-1,3,5,8,10,12-hexaazacyclotetradecane; L^{20} = 3,10-dipropyl-1,3,5,8,10,12-hexaazacyclotetradecane; L^{21} = 1,3,6,8,11,14-hexaazatricyclo(12.2.1.18,11)octadecane; pn = 1,2-propanediamine; tetren = tetraethylenepentaamine; tn = 1,3-propanediamine; tren = tris(2-aminoethyl)amine.

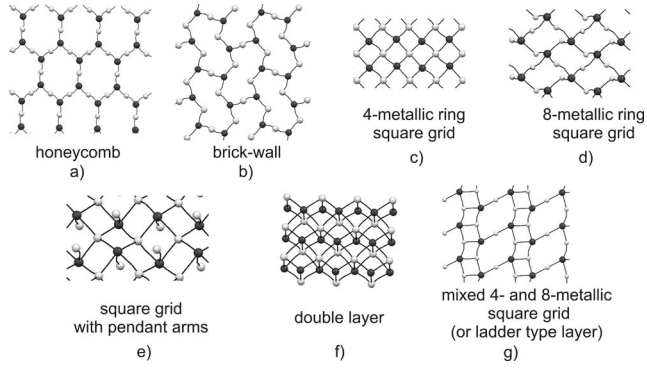

Figure 5. Topological and structural patterns in 2D systems. Dark grey spheres: Mo, W or Nb; light grey spheres: 3d metals; black sticks: CN^- bridges. Blocking and terminal ligands were omitted for clarity.

2.1.4. 3D Assemblies

In comparison to the large variety of low-dimensional structures, there are relatively few types of 3D bimetallic cyanide-bridged assemblies based on octacyanides (Table 4).[16,17,18c,22,23,25,114–127] Most of them are combinations of the $[M^{IV}(CN)_8]^{4-}$ anion with dications, and it is clear that the 1:2 ratio, which is forced by the relative charges of the ions, favours formation of 3D networks. Within the group of compounds of the general formula $\{M^{II}_2[M(CN)_8]\}$, there are two types of structures most commonly observed. When equatorial positions of the cation are blocked and it serves as a linear connector, four of eight cyanide groups of $[M^{IV}(CN)_8]^{4-}$ are engaged in the formation of bridges, which results in loosely packed, diamond-like (Figure 6a)[115–118] or regular (Figure 6b)[22,119,120,122] structures. In the absence of blocking ligands, closely packed networks having all cyanides as bridging ligands are formed (Figure 6c).[16,17,114,121,123–126] They can be described as 2D topologies of the square-grid type joined by the additional cyanide bridges in the third direction. Most commonly, the cation is surrounded by four CN^- bridges in equatorial positions, two axial water molecules making up the octahedral coordination sphere, and the $[M^{IV}(CN)_8]^{4-}$ moiety adopts the shape of square antiprism resulting in high tetragonal symmetry of the networks. This type of network may also be realized by octacyanometallates(V) with some modifications: in $\{[Co^{II}(H_2O)_2]_3[W^V(CN)_8]_2{\cdot}4H_2O\}_n$ two cyanide groups become

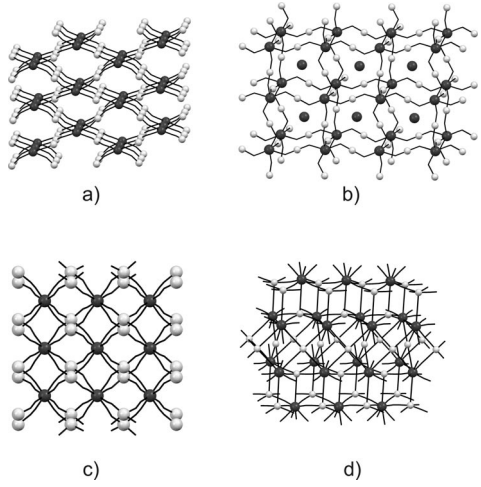

Figure 6. Examples of loosely (a, b) and closely packed (c, d) 3D networks in octacyanometallate-based systems. Dark grey spheres: Mo, W or Nb; light grey spheres: 3d metals; black sticks: CN^- bridges. Blocking and terminal ligands were omitted for clarity.

Table 4. 3D inorganic networks (I^3O^0).[a]

Molecular formula	Number of bridges: $M(CN)_8^{m-}/M'^{n+}$	Ref.
$\{[Ni^{II}(chxn)_2]_2[Mo^{IV}(CN)_8]{\cdot}8H_2O\}_n$	4/2; diamond-like network	[115]
$\{[Ni^{II}(L^{22})]_2[W^{IV}(CN)_8]{\cdot}6H_2O\}_n$		[116]
$\{[Cu^{II}(NH_3)_4]_2[W^{IV}(CN)_8]\}_n$		[117]
$\{[Cu^{II}L^{23}]_2[W^{IV}(CN)_8]{\cdot}4H_2O\}_n$		[118]
$\{[Cu^{II}(en)_2][Cu^{II}(en)][W^{IV}(CN)_8]{\cdot}4H_2O\}_n$	5/3,2	[119]
$\{[Cu^{II}(en)_2]_3[W^V(CN)_8]_2{\cdot}H_2O\}_n$	6,0/2, cube-like	[120]
$\{[M'^{II}(pyr)_4]_2[Nb^{IV}(CN)_8]{\cdot}4H_2O\}_n$ (M′ = Mn, Fe, Co, Ni)	4/2	[22]
$\{[Co^{II}(H_2O)_2]_3[W^V(CN)_8]_2{\cdot}4H_2O\}_n$	6/4, defect tetragonal	[121a]
$\{[Mn^{II}(imH)(H_2O)_2]_2[Nb^{IV}(CN)_8]{\cdot}4H_2O\}_n$	6/3, ladder-type	[23b,25]
λ- and β-$\{[Mn^{II}(urea)_2(H_2O)]_2[Nb^{IV}(CN)_8]\}_n$	6/3	[23c]
$\{Cs^I_2[Cu^{II}(NH_3)_4][Cu^{II}(H_2O)]_2[W^{IV}(CN)_8]_2{\cdot}2H_2O\}_n$	6/5,1	[114,117]
$\{[Mn^{II}(H_2O)]_3[Mn^{II}(H_2O)_2]_3[W^V(CN)_8]_4{\cdot}13H_2O\}_n$	7,6/5,4	[16]
$\{Cu^{II}_{2+x}\{Cu^{II}_4[W^V(CN)_8]_{4-2x}[W^{IV}(CN)_8]_{2x}\}{\cdot}yH_2O\}_n$	8,7/5,4	[18c]
$Cs^I_2Cu^{II}_7[Mo^{IV}(CN)_8]_4{\cdot}6H_2O$	8,7/5,4	[19e]
$[(\{CH_3\}_3Sn)_4M^{IV}(CN)_8]$ (M = Mo, W)	8/2, cube-like	[122]
$\{[Mn^{II}(H_2O)_2]_2[M^{IV}(CN)_8]{\cdot}4H_2O\}_n$ (M = Mo, W, Nb)	8/4, tetragonal	[17,114,123,124]
$\{[Co^{II}(H_2O)_2]_2[M^{IV}(CN)_8]{\cdot}4H_2O\}_n$ (M = W, Nb)	8/4	[121]
$\{[Fe^{II}(H_2O)_2]_2[M^{IV}(CN)_8]{\cdot}4H_2O\}_n$ (M = Mo, W,Nb)	8/4	[125,126]
$\{[Mn^{II}(H_2O)_2]_2[W^{IV}(CN)_8]{\cdot}3H_2O\}_n$	8/4	[114,124]
$[\{Nd^{III}(CH_3OH)_4Mo^{IV}(CN)_8\}_3]^{3-}{\cdot}[Nd^{III}(H_2O)_8]^{3+}{\cdot}8CH_3OH$	4/4	[127]

[a] chxn = cyclohexane-1,2-diamine; en = ethylenediamine; L^{22} = 5,7,7,12,14,14-hexamethyl-1,4,8,11-tetraazacyclotetradecane; L^{23} = 3,10-bis(2-hydroxyethyl)1,3,5,8,10,12-hexaazacyclotetradecane; imH = imidazole; pyr = pyrazole.

Table 5. Hybrid organic–inorganic networks (I^nO^n).[a]

Extended inorganic hybrids, I^nO^0, n = 1, 2, 3 Molecular formula	Hybrid dimensionality	Ref.
$\{(PPh_4)_2[Ru_2(piv)_4(\mu\text{-}CN)W(CN)_7]\}_n$	I^1O^0	[128]
$[\{[Cu_3(L^{24})]_2[W(CN)_8]\}\{W(CN)_8\}](NO_3)_4\cdot 20H_2O$	I^2O^0	[70]
$\{[Mn^{II}_2(H_2O)_2(CH_3COO)][W^V(CN)_8]\cdot 2H_2O\}_n$	I^3O^0	[129]
$\{Cs[Mn^{II}_4(CH_3COO)_3(H_2O)_2][W^V(CN)_8]_2\}_n$	I^3O^0	[129]
$\{Mn^{II}_2(pzdo)(H_2O)_4[Nb^{IV}(CN)_8]\}\cdot 5H_2O$	I^3O^0	[23a]
$\{Mn^{II}_2(bpm)(H_2O)_2[Nb^{IV}(CN)_8]\}$	I^3O^0	[23a]
$[\{Co^{II}(pym)(H_2O)\}_2\{Co^{II}(H_2O)_2\}\{W^V(CN)_8\}_2](pym)_2\cdot 2H_2O$	I^3O^0	[130a,130b]
$\{[Cu_2(H_2Tea)_2]_5[W^V(CN)_8]_2[W^{IV}(CN)_8]\cdot xH_2O\}_\infty$	I^3O^0	[131]
$\{[Cu^{II}(OCH_2CH_2NH_2)_4][M^{IV}(CN)_8]\cdot 2H_2O\}_\infty$	I^3O^0	[132]
Coordination polymers, I^0O^n, n = 1, 2, 3 Molecular formula	Hybrid dimensionality	Ref.
$\{Mn^{II}_9(4,4'\text{-bpy})_4[W^V(CN)_8]_6(CH_3CH_2OH)_{12}(H_2O)_4\}\cdot 10CH_3CH_2OH$	I^0O^2	[26a]
Mixed organic–inorganic hybrids, I^nO^n, n = 1, 2, 3 Molecular formula	Hybrid dimensionality	Ref.
$[Cu(\mu\text{-}4,4'\text{-bpy})(dmf)_2][Cu(\mu\text{-}4,4'\text{-bpy})(dmf)]_2[W^V(CN)_8]_2\cdot 2dmf\cdot 2H_2O$	I^1O^1	[20]
$\{Co^{II}_3(H_2O)_6(pyz)_3[W^V(CN)_8]_2\}\cdot 3.5H_2O$	I^1O^1	[133]
$\{Co^{II}_3(H_2O)_4(4,4'\text{-bpy})_3[W^V(CN)_8]_2\}\cdot 1.5(4,4'\text{-bpy})\cdot 6H_2O$	I^1O^1	[133]
$\{[Ce_2(bpm)(dmf)_8(H_2O)_2][W(CN)_8]_2\}_n\cdot 2nH_2O$	I^1O^1	[45]
$\{Mn^{II}_9(dpe)_5[W^V(CN)_8]_6(CH_3OH_{10})\}\cdot 14CH_3OH$	I^1O^2	[26b]
$[Ln^{III}(mpca)_2(H_2O)(CH_3OH)Ln^{III}(H_2O)_6W^{IV}(CN)_8]_3\cdot nH_2O$ (Ln = Eu, Nd)	I^2O^1	[134]
$[Tb(H_2O)_4(pyz)_{0.5}]W(CN)_8$	I^2O^1	[135]
$\{[\mu_4\text{-}M(CN)_8]Cu_2(dpp)_4\}_n$	I^2O^2	[136]
$\{Mn^{II}_2(pyz)_2(H_2O)_4[Nb^{IV}(CN)_8]\}\cdot pyz\cdot 3H_2O$	I^3O^1	[23a]
$[\{Mn^{II}(pyz)(H_2O)_2\}\{Mn^{II}(H_2O)_2\}\{M^{IV}(CN)_8\}]\cdot 4H_2O$ (M = Mo, Nb)	I^3O^1	[137,138,139]
$[\{Mn^{II}(pym)(H_2O)\}_2\{Mn^{II}(H_2O)_2\}\{W^V(CN)_8\}_2](pym)_2\cdot 2H_2O$	I^3O^1	[140]
$Cu^{II}_3[W^V(CN)_8]_2(pym)_2\cdot(CH_3)_2CHOH\cdot 6H_2O$	I^3O^1	[141]
$Cu^{II}_3[W^V(CN)_8]_2(pym)_2\cdot CH_3CH_2CH(OH)CH_3\cdot 5H_2O$	I^3O^1	[141]
$Cu_3[W(CN)_8]_2(pym)_2\cdot 8H_2O$	I^3O^1	[142]

[a] 4,4′-bpy = 4,4′-bipyridine; bpm = 2,2-bipyrimidine; dmf = *N*,*N*-dimethylformamide; dpe = 1,2-bis(4-pyridyl)ethylene; dpp = 1,3-bis(4-pyridyl)propane; L^{24} = 1,3,5-triazine-2,4,6-triyltris[3-(1,3,5,8,12-pentaazacyclotetradecane)]; mpca = 5-methyl-2-pyrazinecarboxylic acid; piv = pivalate anion; pym = pyrimidine; pyz = pyrazine; pzdo = pyrazine-*N*,*N*′-dioxide; Tea = triethanolamine.

terminal, as if one fourth of the cations were missing,[121] while in hybrid $\{[Mn^{II}_2(H_2O)_2(CH_3COO)][W^V(CN)_8]\cdot 2H_2O\}_n$ (see Table 5) the 2:1 ratio is achieved by the presence of the charged bridging acetate ligand. Most of the other known 3D networks show complicated structures with cations and/or anions in two nonequivalent surroundings.[127] Recently we presented an interesting example of the extension of a 2D double layer $\{(dienH_3)Cu^{II}_3[M^V(CN)_8]\cdot 4H_2O\}_n$ toward the related 3D $\{Cu^{II}_{2+x}\{Cu^{II}_4[W^V(CN)_8]_{4-2x}[W^{IV}(CN)_8]_{2x}\}\cdot yH_2O\}_n$ network with additional cyanide-bridged interlayer copper(II) cations (Figure 6d).[18c,19d,19e]

2.2. Mixed Organic–Inorganic Hybrid Networks

Organic–inorganic hybrid networks based on octacyanometallates[20,23a,26,45,70,128–142] together with the generalized Cheetham notation[28] are summarized in Table 5.

The first hybrid system based on octacyanometallates is the 2D I^1O^1 $[Cu(\mu\text{-}4,4'\text{-bpy})(dmf)_2][Cu(\mu\text{-}4,4'\text{-bpy})(dmf)]_2[W^V(CN)_8]_2\cdot 2dmf\cdot 2H_2O$ (Figure 7a). Its structure can be interpreted as cross-linking chains: Cu_3W_2 cyanide-bridged chain of 3,2-chain topology and $\{Cu(\mu\text{-}4,4'\text{-bpy})\}$ linear chains.[20] An interesting example of coordination isomerism can be observed for two Mn-pyz-Nb hybrid systems, which together constitute the first examples of the new I^3O^1 class of networks, although they present different topologies. The molecular structure of $[\{Mn^{II}(pyz)(H_2O)_2\}\{Mn^{II}(H_2O)_2\}\{Nb^{IV}(CN)_8\}]\cdot 4H_2O$ consists of cyanide-bridged Mn–Nb square grids bridged with the interplanar Mn centres involved also in $\{Mn(\mu\text{-}pyz)\}_n$ chains running between these layers (Figure 7b).[137,138] On the contrary, $\{Mn^{II}_2(pyz)_2(H_2O)_4[Nb^{IV}(CN)_8]\}\cdot pyz\cdot 3H_2O$ consists of ladder-type cyanide-bridged Mn-Nb$(CN)_8$ layers connected by $[Mn\text{-}(\mu\text{-}pyz)]^{2+}$ chains and by $[Mn\text{-}(\mu\text{-}CN)]^+$ chains cross-linking between the layers (Figure 7c).[23a] Both isomers are soft ferrimagnets with T_c values of 48 K and 27 K, respectively. $[\{Mn^{II}(pyz)(H_2O)_2\}\{Mn^{II}(H_2O)_2\}\{Nb^{IV}(CN)_8\}]\cdot 4H_2O$ crystallizes in an acentric space group and reveals MSHG below the ordering temperature.[139]

In our very recent contributions we tested successfully the pentadecanuclear cluster $\{Mn_9W_6\}$ (see Figure 2b)[14,15] as the novel cyanide-bridged secondary building block (SBB) in the construction of new extended hybrid systems. The essential prerequisite for its application is the simultaneous presence of geometrically arranged acidic coordination sites, *fac*-$[Mn^{II}(\mu\text{-}NC)_3(solv)_3]$, and a basic coordination function, $[M^V(\mu\text{-}CN)_5(CN)_3]$, in specific external parts of the cluster. The slow diffusion of in situ formed $\{Mn_9W_6\}$ clusters and 4,4′-bpy in alcoholic media gave

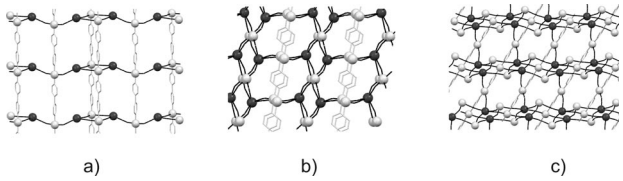

Figure 7. Examples of coordination frameworks of mixed organic–inorganic hybrids: $[Cu(\mu\text{-}4,4'\text{-bpy})(dmf)_2][Cu(\mu\text{-}4,4'\text{-bpy})(dmf)]_2[W^V(CN)_8]_2\cdot 2dmf\cdot 2H_2O$ (I^1O^1) (a); different types of cross-linking between {Mn-(μ-pz)} chain and 3D cyanide-bridged network in two Mn^{II}-pyz-$[Nb^{IV}(CN)_8]^{4-}$ coordination isomers (I^3O^1) (b) and (c). Dark grey spheres: Mo, W or Nb; light grey spheres: 3d metals; black sticks: CN^- bridges, light grey sticks: organic linkers. Blocking and terminal ligands were omitted for clarity.

$\{Mn^{II}_9(4,4'\text{-bpy})_4[W^V(CN)_8]_6(EtOH)_{12}(H_2O)_4\}\cdot 10EtOH$, in which $\{Mn_9W_6\}$ clusters are linked into the 2D I^0O^2 network by the 4,4′-bpy ligands (Figure 8a).[26a] The use of a longer bis(pyridyl)dpe ligands produced the unprecedented architecture $\{Mn^{II}_9(dpe)_5[W^V(CN)_8]_6(MeOH)_{10}\}\cdot 14MeOH$ revealing I^1O^2 topology, in which $\{Mn_9W_6\}$ clusters are connected by quadruple sets of cyanide bridges to the nanotubes $\{Mn_9W_6\}_n$, which are further organized into 3D structure by dpe ligands (Figure 8b).[26b] Within the former network, the clusters retain their magnetic identity,[14a,15] while in the latter long-range magnetic ordering appears with decreasing temperature: first within the $\{Mn_9W_6\}_n$ skeletons, then in the bulk crystals.

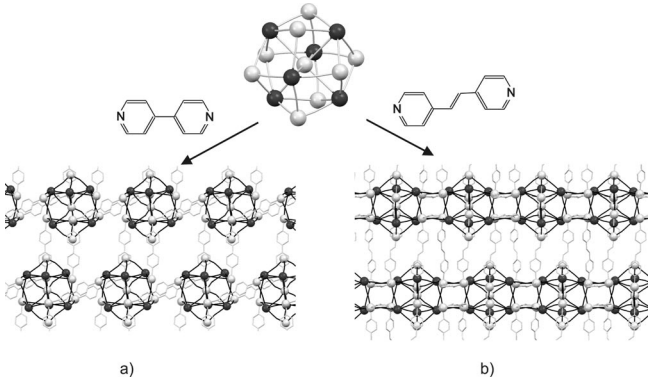

Figure 8. Crystal engineering of $Mn^{II}_9W^V_6$ clusters into coordination polymers (I^0O^2) (a) and into mixed organic–inorganic hybrids (I^1O^2) (b). Dark grey spheres:W; light grey spheres: Mn^{II}; black sticks: CN^- bridges, light grey sticks: organic linkers. Blocking and terminal ligands were omitted for clarity.

A very interesting example of crystal engineering is the encapsulation of $[M^{IV}(NC)_8]^{4-}$ (M = Mo, W) by a tricopper(II) complex with triple macrocyclic L ligands (Figure 9). Prepared in that way, assemblies may coordinate nitrate anions or additional $[M^{IV}(CN)_8]^{4-}$ anions at the external axial position of Cu^{II} complexes to give a discrete architecture or extended network, respectively.[70]

Lanthanide ions characterized by large coordination numbers easily adapt to the surroundings, allowing the observation of very unusual examples of crystal engineering of bimetallic hybrid networks. We observed growth of crystals starting from cerium(III) nitrate, sodium octacyanotungstate(V) and 2,2′-bipyrimidine (bpm),[45] which depended strongly on the reaction conditions. In water/dmf solution (dmf = *N*,*N*-dimethylformamide) layered with CH_3CN, ionic $[Ce_2(bpm)(dmf)_6(H_2O)_8][W(CN)_8]_2\cdot 3H_2O$ with Ce^{III}–bpm–Ce^{III} linkages was formed. The concentration of a water/dmso solution gave tetranuclear molecules of $[Ce_2(bpm)(dmso)_8(H_2O)_4][W(CN)_8]_2\cdot 4H_2O$ I^0O^0, while isolation by concentration from CH_3OH/dmf mixture gave a 2D organic–inorganic hybrid (I^1O^1) $\{[Ce_2(bpm)(dmf)_8(H_2O)_2][W(CN)_8]_2\}_n\cdot 2nH_2O$, both of them with W^V–CN–Ce^{III} and Ce^{III}–bpm–Ce^{III} linkages (Figure 10a).[45] The last compound is the clear extension of simple 1D $Ln^{III}M^V$ chains reported in previous sections. Similarly, the layering of pyrazine vapour on the partially dehydrated solid of $\{[Tb(H_2O)_4][W(CN)_8]\}_n$ with a square grid reported by Song at al. leads to the formation of the 3D $\{[Tb(H_2O)_4(pyrazine)_{0.5}][W(CN)_8]\}_n$ hybrid network in which pyrazine links the neighbouring grids (Figure 10b).[135]

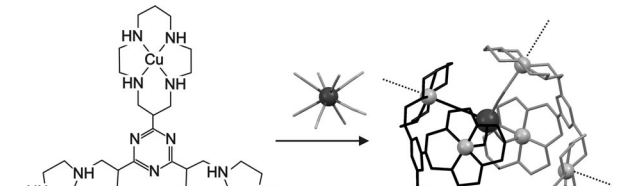

Figure 9. The encapsulation of $[M^{IV}(CN)_8]$ by two units of Cu_3L. Dotted lines indicate the axial coordination sites at Cu^{II} centres. Dark grey spheres: Mo, W; light grey spheres: 3d metals.

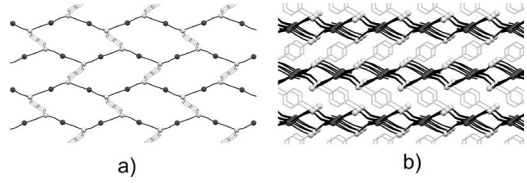

Figure 10. Lanthanide–octacyanometallate mixed organic–inorganic hybrid networks: $\{[Ce_2(bpm)][W(CN)_8]_2\}_n$ (I^1O^1) developing 1D chains (I^1O^0) (a) and $\{[Tb(H_2O)_4(pyrazine)_{0.5}][W(CN)_8]\}$ (I^2O^1) developing 2D square grids (I^2O^0) (b). Dark grey spheres: W; light grey spheres: Ce^{III} or Tb^{III}; black sticks: CN^- bridges, light grey sticks: organic linkers. Blocking and terminal ligands were omitted for clarity.

3. Functionality

3.1. Photomagnetism

Photomagnetism is one of the most desired properties for molecular materials, in view of the perspectives of fast light-induced conversion between different spin states. Since the discovery of the photomagnetic effect in 1996 in cobalt–iron Prussian blue analogues,[143] a great deal of work has been done in the field of cyanide-bridged photomagnetic materials.[2a]

In the case of octacyanometallate-based systems, one of the first photomagnetic studies concerned low-dimensional

paramagnetic systems with Mn^{II}–NC–Mo^{IV} and Mn^{II}–NC–W^{IV} linkages. The group of Mathoniere and Kahn reported photomagnetic studies on the 1D chain $[Mn^{II}_2(L^{14})_2(H_2O)][Mo^{IV}(CN)_8]\cdot 5H_2O$. Under laser irradiation (λ = 336–357 nm, T = 10 K) in the SQUID cavity, irreversible photooxidation was observed, which resulted in the formation of material with antiferromagnetic coupling between Mn^{II} and Mo^{V} through cyanide bridges.[73] Continuing this line of research, we investigated the photomagnetic properties of hexanuclear cluster $[Mn^{II}(bpy)_2]_4[M^{IV}(CN)_8]_2\cdot xH_2O$ (M = Mo, x = 14, and M = W, x = 9) (Figure 2a).[21] Irradiation under similar conditions led to the increase of the magnetic signal by a factor of almost 30% relative to that of the initial material. This change was interpreted in terms of the formation of $Mn^{II}_2Mn^{I}_2M^{V}_2$ due to the reductive quenching of the excited intraligand 2,2-bpy-centred state in $Mn^{II}_4M^{IV}_2$ through an intramolecular electron-transfer mechanism. The shape of the $\chi T(T)$ curves indicated intermetallic exchange coupling through metallic centres. Complete thermal reversibility of the photomagnetic process was observed in the case of the $Mn^{II}_4W^{IV}_2$ system, while in the case of $Mn^{II}_4Mo^{IV}_2$, the reversibility was incomplete.

Parallel to this research, the extended studies done in the groups of Hashimoto, Ohkoshi, Mathoniere and Marvaud focused around the photoswitchable, solid-state $\{Cu^{II}[Mo^{IV}(CN)_8]\}$[19e,37,38,50,51,93,107,144–148] and $\{(HS)Co^{II}[W^{V}(CN)_8]\}$[99,130,133,149–155] systems revealing MMCT characteristics in the spectral UV/Vis/NIR region. 3D system $Cu^{II}_2[Mo^{IV}(CN)_8]\cdot 8H_2O$ exhibits photoinduced charge transfer ($\lambda_{max} \approx 480$ nm), producing $Cu^{I}Cu^{II}[Mo^{V}(CN)_8]\cdot 8H_2O$ with ferromagnetic ordering below T_c = 20 K due to the exchange interactions between Cu^{II} and Mo^{V} centres. This process can be reversed either by thermal treatment or by irradiation at the reverse IT (intervalence transfer) band (λ = 600–900 nm).[144,145] Other examples of photomagnetic polymers containing Cu and Mo centres are the 3D $Cs_2Cu_7[Mo(CN)_8]_4\cdot 6H_2O$,[19e] the 2D $[CuL]_2[Mo(CN)_8]\cdot 10H_2O$, where L = cyclam,[107] and the 1D heterotrimetallic chain $[(Ni(cyclam))(Mo(CN)_8)_2(Cu(Me_2en)_2)_7](ClO_4)_8\cdot 4H_2O$.[93] All these systems exhibit ferromagnetic coupling between Mo^{V} and Cu^{II} after photoinduced charge transfer.

A similar mechanism is used to explain the photoinduced magnetic properties of the following 0D oligonuclear assemblies: pentanuclear $[Mo(CN)_8\{CuL^8\}_2\{CuL^8(H_2O)\}_2]\cdot 6H_2O$, decanuclear $[Mo(CN)_8\{CuL^9\}_3\{CuL^9(H_2O)\}]_2\cdot 10H_2O$[50] and heptanuclear $[Mo(CN)_2(CN\text{-}Cutren)_6](ClO_4)_8\cdot 4.5H_2O$.[51] For the last system, detailed theoretical and kinetic models have been developed, by taking into account the contribution of the excited states of the molybdenum ion in the photomagnetic process.[146–148]

Combination of $(HS)Co^{II}$ and $[W^{V}(CN)_8]^{3-}$ centres yielded the 2D compound $Cs^{I}[\{Co^{II}(3\text{-cyanopyridine})_2\}\{W^{V}(CN)_8\}]\cdot H_2O$, which exhibited a temperature-induced phase transition between Co^{II}–W^{V} (HT phase) and Co^{III}–W^{IV} (LT phase) isomers with a large thermal hysteresis between 165 and 216 K as well as photoinduced magnetization ($\lambda \approx 800$–900 nm) in the low-temperature metastable state with T_c = 30 K.[99] Analogous but nonstoichiometric compounds with metal vacancies were investigated earlier by means of XANES (X-ray absorption near edge structure) analysis, with similar conclusions confirming the oxidation states of the HT, LT and photoinduced phases.[149,150] Studies of this system were further extended to the analysis of the relaxation kinetics of the metastable phase induced by rapid cooling of HT phases as well as by irradiation of the LT phase at low temperature.[151] For 3D $Co^{II}_3[W^{V}(CN)_8]_2(pyrimidine)_4\cdot 6H_2O$, temperature-induced transition between Co^{II}–W^{V} (HT phase) and Co^{III}–W^{IV} (LT phase) isomers revealed a large thermal hysteresis covering the room temperature region (between 210 and 300 K) and photoinduced magnetization in the low-temperature metastable state with T_c = 40 K.[130a] Further investigation proved the photorevesibility of the excitation process as well as confirming ferromagnetic interactions between W^{V} and Co^{II} centres.[130b] Moreover, the recent study of this system by the group of Bousseksou led to the discovery of a new phenomenon: Electric-Field-Induced Charge-Transfer Phase Transition.[152]

Other attempts to connect Co and W centres with organic ligands were made in our group, resulting in the ferromagnet $\{Co^{II}_3(H_2O)_6(pyz)_3[W^{V}(CN)_8]_2\}\cdot 3.5H_2O$ (T_c = 26 K) and $Co^{II}_3(H_2O)_4(4,4'\text{-bpy})_3[W^{V}(CN)_8]_2\cdot 1,5(4,4'\text{-bpy})\cdot 6H_2O$, which shows glass-like magnetic phase transition below T_G = 16 K.[133] These compounds did not undergo thermally induced electron transfer; however, preliminary photomagnetic studies at low temperature with a green laser (λ = 532 nm) revealed a significant photomagnetic effect interpreted in terms of the reverse $Co^{II}W^{V} \rightarrow Co^{III}W^{IV}$ transition.[153]

Very recently we have shown that a change in magnetic properties may be induced by photostimulation of $[M(bpy)_3]^{n+}[Mo(CN)_8]^{4-}$ (M = Ni^{II}, Co^{III}) ionic compounds. The significant increase of the paramagnetic signal under light irradiation was observed for $[Ni(bpy)_3]_2[Mo^{IV}(CN)_8]\cdot 12H_2O$[154] and for the dehydrated phase of $K[Co(bpy)_3][Mo(CN)_8]\cdot 8H_2O$.[155] In both cases, photoinduced metastable phases were observed, relaxing to the initial states at temperatures of approximately 240 and 290 K, respectively.

3.2. Tuning of T_c

Octacyanometallates are suitable building blocks for construction of networks with long-range magnetic ordering.[16,17,22–25,99,106,110–112,121,126,127,130,134,138–142] The tuning of critical temperatures, T_c, may be particularly realized in networks of the general formula $\{M'_x(L)_n[M(CN)_8]_y\cdot zH_2O\}_n$.[22,23,25] by changing: (1) the magnetic centres M and M′, (2) the organic ligand L and (3) the degree of hydration (or more generally solvation). In order to investigate the possibilities to tune the T_c we have investigated three series of compounds including: (1) four isomorphic magnets $\{[M'^{II}(pyrazole)_4]_2[Nb^{IV}(CN)_8]\cdot 4H_2O\}_n$, where M′ = Mn, Fe, Co, Ni; (2) four topologically identical magnets incorporating different organic ligands L,

$\{[Mn^{II}(imH)(H_2O)_2]_2[Nb^{IV}(CN)_8]\cdot 4H_2O\}_n$ (imH = imidazole), $\{Mn^{II}_2(pzdo)(H_2O)_4[Nb^{IV}(CN)_8]\cdot 5H_2O\}_n$ (pzdo = pyrazine dioxide) and two polymorphs of $\{[Mn^{II}(urea)_2(H_2O)]_2[Nb^{IV}(CN)_8]\}_n$ and (3) products of chemical modifications of selected networks. The changes of the critical temperatures within the particular group can be roughly explained by using molecular field theory [Equation (1)].

$$T_c = \frac{2\sqrt{n_M n_{M'}}\,|J_{MM'}|\sqrt{S_M(S_M+1)S_{M'}(S_{M'}+1)}}{3k_B} \quad (1)$$

In this equation, n_M is the number of the nearest magnetic neighbours bridged to the octacyanometallate M centre, $n_{M'}$ is the number of the nearest magnetic neighbours bridged to the M′ centre, $J_{MM'}$ is the magnetic coupling constant present in the Hamiltonian describing the magnetic interaction between two metal centres proposed by Heisenberg and discussed by Dirac and Van Vleck ($\mathbf{H} = -J_{MM'}\,S_M.\,S_{M'}$), S_M is the effective spin of M (usually 1/2), $S_{M'}$ is the effective spin of M′ and k_B is the Boltzmann constant, which is equal to 0.69372 $cm^{-1}\,K^{-1}$.[156,157]

We have recently shown that the use of different paramagnetic centres M and M′ influence mainly the strength of the interaction and the value of the coupling constant $J_{MM'}$.[22] For the series of isostructural compounds of general formula $\{[M'^{II}(pyrazole)_4]_2[Nb^{IV}(CN)_8]\cdot 4H_2O\}_n$ (Figure 11a), it was found that the coupling constants $J_{NbM'}$ increase on going from Mn^{II} to Ni^{II} with a change in the character of the magnetic interaction from antiferromagnetic for Mn^{II} and Fe^{II} to ferromagnetic for Co^{II} and Ni^{II}. Careful magnetostructural analysis of the relation between the decreasing number of unpaired electrons on the M′ centre and the increasing value of exchange coupling revealed the presence of two main contributions to the total exchange coupling J_{MNb}: an antiferromagnetic part originating from t_{2g} orbitals of the M′ centre (with an average value of –21.6 cm^{-1}) and a ferromagnetic part originating from its e_g orbitals (J_F = 15.4 cm^{-1}), which is in agreement with Kahn's model of interaction.[158] The antiferromagnetic contribution is successively weakened with each additional electron on the t_{2g} level in the $Mn^{II} > Fe^{II} > Co^{II} > Ni^{II}$ sequence, which results in a variation in the strength and character of the exchange coupling between M′ and Nb^{IV} and in the nature of the long-range magnetic ordering. It is worth noting that the values of the averaged contributions can be used to predict the total exchange integrals for not yet reported possible members of the $\{[M'^{II}(pyrazole)_4]_2[Nb^{IV}(CN)_8]\cdot 4H_2O\}_n$ family with M′ = Cr^{II} or V^{II}. For the Cr^{II}-based analogue J_{CrNb} should be close to –12 cm^{-1}, and for the V^{II} analogue the prediction for J_{VNb} is –17 cm^{-1} (Figure 11b).

Changing the M centre of the octacyanometallate moiety can cause extremely drastic changes in the magnetic properties. For example, the replacement of the paramagnetic $[Nb^{IV}(CN)_8]^{4-}$ in the ferrimagnetic inorganic network $\{[Mn^{II}(H_2O)_2]_2[Nb^{IV}(CN)_8]\cdot 4H_2O\}_n$ (T_c = 43 K) by its diamagnetic relatives $[Mo^{IV}(CN)_8]^{4-}$ and $[W^{IV}(CN)_8]^{4-}$ leads to

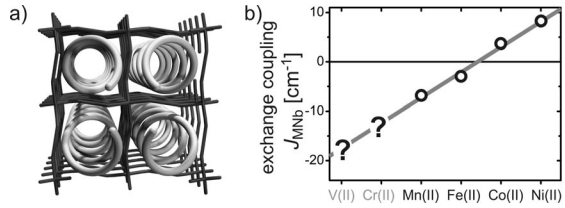

Figure 11. Schematic representation of the structure of the $\{[M'^{II}(pyrazole)_4]_2[Nb^{IV}(CN)_8]\cdot 4H_2O\}_n$ family (black sticks: cyanide skeleton, grey helices: pyrazole superstructures) (a); linear dependence of the coupling constant J_{MNb} in the row of 3d transition metal M^{2+} ions (b).

simple isostructural paramagnetic solids, as shown by Verdaguer et al. and Ohkoshi et al. in the series of three isostructural compounds $\{[Mn^{II}(H_2O)_2]_2[M^{IV}(CN)_8]\cdot 4H_2O\}_n$, where M = Nb, Mo or W.[123,17]

The influence of organic ligands on the magnetic properties of octacyanometallate-based compounds must be considered in view of a few aspects including: coordination mode (bridging, blocking) and involvement in weak supramolecular interactions (e.g. hydrogen bonding, π–π stacking). If organic molecules play the role of blocking ligands coordinated to the M′, they simply isolate the magnetic centres from each other and reduce the connectivity of the resulting network, and thus the number of the nearest neighbours n in Equation (1). In such cases, the critical temperatures of the magnetic transitions are usually lowered in comparison to that of the purely inorganic "parent" framework, while the topology becomes much more complicated.

In order to gain some deeper insight into the role of the incorporated organic ligands on the magnetic properties, we analyzed four topologically identical 3D hybrid networks with different organic components. Recently we have shown that three Mn^{II}_2–L–$Nb^{IV}(CN)_8$ compounds, $\{[Mn^{II}(imH)(H_2O)_2]_2[Nb^{IV}(CN)_8]\cdot 4H_2O\}_n$ (**A**), $\{Mn^{II}_2(pzdo)(H_2O)_4[Nb^{IV}(CN)_8]\cdot 5H_2O\}_n$ (**B**) and two polymorphs of $\{[Mn^{II}(urea)_2(H_2O)]_2[Nb^{IV}(CN)_8]\}_n$ (**C1**/**C2**, α/β), exhibit identical 6:3 connectivity with nearest neighbour numbers n_{Mn} = 3 and n_{Nb} = 6 and very similar crossed-ladder-type topology (Figure 12).[23,25]

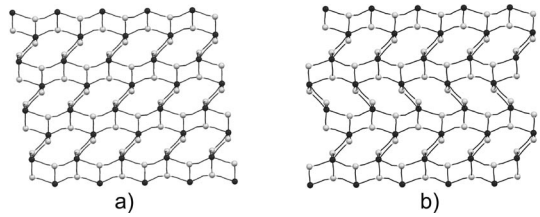

Figure 12. 3D ladder type topology in $\{[Mn^{II}(imH)(H_2O)_2]_2[Nb^{IV}(CN)_8]\cdot 4H_2O\}_n$, $\{Mn^{II}_2(pzdo)(H_2O)_4[Nb^{IV}(CN)_8]\cdot 5H_2O\}_n$, β-$\{[Mn^{II}(urea)_2(H_2O)]_2[Nb^{IV}(CN)_8]\}_n$ (a) and α-$\{[Mn^{II}(urea)_2(H_2O)]_2[Nb^{IV}(CN)_8]\}_n$ (b). Dark grey spheres: Nb; light grey spheres: Mn; black sticks: CN^- bridges.

Moreover **A**, **B**, **C2** and **C1** are all soft ferrimagnets showing very much the same magnetic behaviour but different values of critical temperatures, T_c, of 25, 37, 42 and 43 K, respectively. At first glance, the incorporated organic

ligands L in this series seem to have rather negligible influence on the magnetic interactions, because they are diamagnetic and act more as blocking ligands. Closer analysis, however, reveals that they must influence the magnetic properties indirectly. In fact, their presence in the soft crystal lattice and their ability to form weak hydrogen bonds or engage in π–π interactions alter the nonrigid geometry of $[Nb^{IV}(CN)_8]$ moieties and the characteristics of cyanide bridges. Sutter et al.[34] showed that the spin density delocalized on the N atoms of the paramagnetic $[Mo^{V}(CN)_8]^{3-}$ complex {which is isoelectronic with $[Nb^{IV}(CN)_8]^{4-}$} is strongly dependent on its coordination geometry. For the dodecahedral (DD) geometry, the spin density delocalized on N atoms placed in "B vertexes" is found to be almost three times larger than those placed in "A vertexes". For the square antiprism (SAPR) geometry, all CN^- ligands of the $[M(CN)_8]$ moiety are equivalent, and the spin density delocalized on all eight N atoms is the same. Moreover, it was shown that the spin density on N atoms for SAPR is about 35% lower than the spin found on the $N_{B\text{-vertex}}$ atoms in DD but larger than those for the $N_{A\text{-vertex}}$ sites. Therefore, for the $[M(CN)_8]^{n-}$ moieties (M = Mo^V, W^V, Nb^{IV}), the amount of spin density borne by the CN^- ligands follows the decreasing order $DD_{B\text{-vertex}} > SAPR > DD_{A\text{-vertex}}$, and hence the magnetic coupling constants, *J*, and the magnetic ordering temperatures, T_c, of $[M(CN)_8]$-based compounds should follow the same trend. Compounds **A**, **B** and **C** follow the $DD_{B\text{-vertex}} > SAPR > DD_{A\text{-vertex}}$ rule perfectly (Figure 13). In **C1**, the geometry of $[Nb^{IV}(CN)_8]$ is almost perfectly dodecahedral with four of the cyanide bridges placed in "B vertexes" and only two in "A vertexes" (Figure 13a). In this case, the expected spin density is maximized on the bridging cyanides and T_c is 43 K. In **C2** the situation is very similar (Figure 13b), and the slightly lower value of T_c can be attributed to $[Nb^{IV}(CN)_8]$ geometry slightly more distorted towards SAPR. In **B** there are also four cyanide bridges in "B vertexes" and two in "A vertexes" (Figure 13c), but the geometry of $[Nb^{IV}(CN)_8]^{4-}$ is mixed (DD/SAPR). Hence, the expected spin density should be lower. The observed T_c of 37 K is in fact lower than that in **C**, because of the larger contribution of SAPR geometry in the octacyanoniobate(IV) moiety. The geometry of $[Nb^{IV}(CN)_8]$ in **A** is mixed (DD/SAPR) like that in **B**, but four of the bridging cyanides are placed in "A vertexes" and only two are in "B vertexes" (Figure 13d). Therefore, the expected spin density delocalized on the N atoms is relatively low and the ordering temperature, T_c, is only 25 K.

The incorporated organic molecules in the series **A**–**C** do not change their overall "crossed-ladder" topology nor their connectivity (6:3 in all members), but they do alter the geometry of $[Nb^{IV}(CN)_8]$ moieties and the characteristics of cyanide bridges and in this very subtle way influence indirectly the magnetic properties of this series. The nonrigid geometry of the $[Nb(CN)_8]$ moiety is one of the main factors directly responsible for the T_c value in the octacyanometallate-based hybrid compounds and can be used for efficient tuning of the magnetic interactions. This particular dependence is not observed for the series of compounds based on geometrically rigid hexacyanometallates studied before.[159]

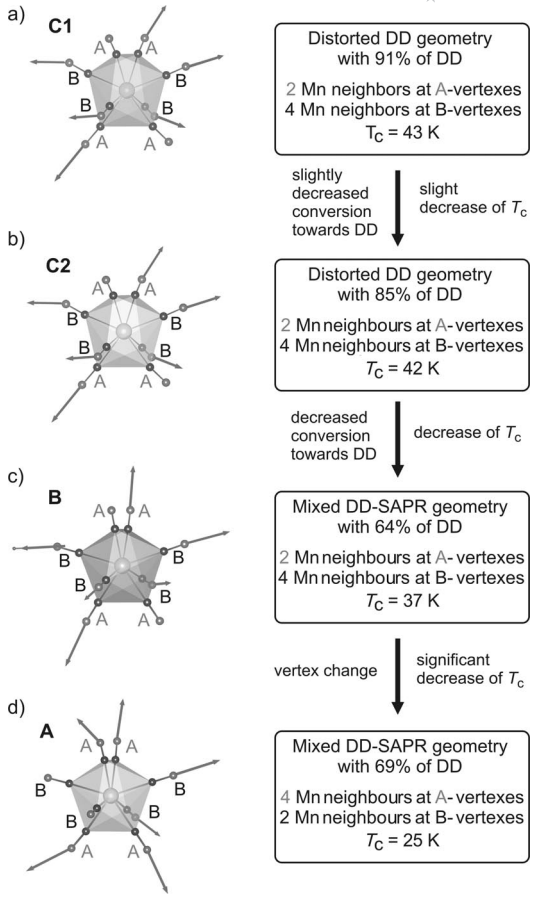

Figure 13. Influence of the $[Nb(CN)_8]$ geometry and the position of bridging cyanide ligands in **C1** (a), **C2** (b), **B** (c) and **A** (d) (indicated by arrows) on the value of critical temperatures T_c (for details, see description in the text).

3.3. Guest-Responsive Molecular Magnets

Engineering and characterization of guest-responsive molecular magnets is a challenging task because of the dynamic character of the changes, which take place upon removal and insertion of guest molecules. Soft crystal frameworks of molecular solids very often fall apart when subjected to high temperatures or very low pressures, while the aim of their engineering is to obtain systems which will show reversibility and durability.[10b,23c,24,25,141,142]

During our continuous study, we managed to obtain and characterize several dynamic systems that can be counted among guest-responsive molecular magnets. Recently we have presented a 2D system based on octacyanotungstate(V) and a nickel(II) cyclam complex: $\{[Ni(cyclam)]_3[W(CN)_8]_2\}_n$ (**D**).[24] Its microporous structure enables reversible adsorption of water into the empty channels across the honeycomb-like planes at ambient conditions (Figure 14). The guest inclusion does not directly influence the coordi-

nation sphere or connectivity, and the process is realized with retention of the crystalline form. It is the first and only example of an octacyanometallate-based microporous network undergoing single-crystal-to-single-crystal transformation. The changes in the geometry of cyanide bridges, which accompany hydration, influence the magnetic exchange between Ni and W, which is reflected in the increase of T_N from 4.9 K for the anhydrous **D** to 8.3 K for the hydrated **D1** form.

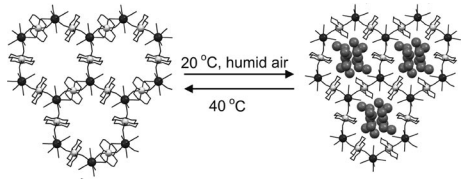

Figure 14. Reversible structure adaptation upon adsorption of water into the empty channels of $\{[Ni(cyclam)]_3[W(CN)_8]_2\}_n$. Dark grey spheres: W; light grey spheres: Ni^{II}; black sticks: CN^- bridges and cyclam, grey spheres: O of H_2O.

The dehydration of 3D $\{[Mn^{II}(imH)(H_2O)_2]_2[Nb^{IV}(CN)_8]\cdot 4H_2O\}_n$ (**A**) leads to a novel molecular magnet $\{[Mn^{II}(imH)]_2[Nb^{IV}(CN)_8]\}_n$ (**A1**), which can be transformed back to **A** upon rehydration (Figure 15).[25] This dynamic sponge-like system exhibits: (1) changeable topology, (2) changeable number of cyanide bridges per $[Nb(CN)_8]$ unit and (3) changeable coordination number and geometry of the Mn^{II} centres. The solid–solid transformation in this system reveals the features of a topotactic reaction, in which hydrogen-bonded H_2O molecules play a key role in the formation/cleavage of the seventh Nb^{IV}–CN–Mn^{II} linkage. The **A**–**A1** structural transformation has tremendous impact on the magnetic behaviour of the system, which is manifested through a significant increase in the ordering temperature from 25 to 62 K and appearance of magnetic hysteresis in **A1**.

Another very interesting example of guest-induced magnetostructural changes can be found in the behaviour of both polymorphs of $\{[Mn^{II}(urea)_2(H_2O)]_2[Nb^{IV}(CN)_8]\}_n$ (**C**).[23c] In this case, however, the observed transformations are irreversible, which is probably caused by the collapse of the crystal network upon guest-molecule extraction. The behaviour of **C** relies on the lability of the urea ligands,

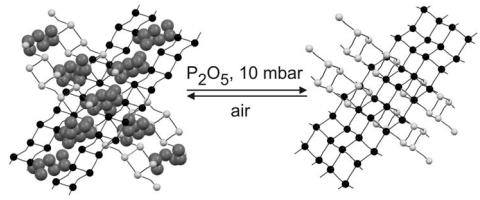

Figure 15. Reversible dehydration of $\{[Mn^{II}(imH)(H_2O)_2]_2[Nb^{IV}(CN)_8]\cdot 4H_2O\}_n$. Dark grey spheres: Nb and Mn in one set of ladders; light grey spheres: Nb and Mn in the second set of ladders; black sticks: CN^- bridges, grey spheres: O of H_2O.

which can be removed very easily. In methanol, **C** transforms into a new compound, $\{[Mn^{II}(H_2O)]_2[Nb^{IV}(CN)_8]\cdot 4MeOH\}_n$ (**Ca**), in which methanol replaces urea. Compound **Ca**, upon hydration, can be further transformed into $\{[Mn^{II}(H_2O)_2]_2[Nb^{IV}(CN)_8]\cdot 4H_2O\}_n$ (**Cb**) (Scheme 1), obtained and characterized before.[17,123] Both polymorphs **C** can also be directly transformed into **Cb** when treated with water.

The values of magnetic ordering temperatures T_c of the $\{[Mn^{II}(urea)_2(H_2O)]_2[Nb^{IV}(CN)_8]\}_n$ molecular system vary from 43/42 K [for both respective polymorphs **C**] through 70 K (for **Ca**) and back to 48 K (for **Cb**) depending on the structural transformations **C**→**Ca**→**Cb**, but its soft ferrimagnetic character remains intact. Again, the changes of the critical temperatures can be explained by utilizing molecular field theory [Equation (1)].

The significant increase in T_c at the first stage of transformation **C**→**Ca** is caused most probably by the increase of the connectivity type (which is equivalent to the increase of the number of nearest neighbours n_{Nb} and n_{Mn}) and the decrease of the coordination number of manganese(II) (which is strongly correlated with the increase in the absolute value of J_{MnNb} from –10.9 cm^{-1} for **C** to –15.1 cm^{-1} for **Ca**, estimated by using a high-temperature mean-field model for the two sublattices).[22,23c]

At the second stage (**Ca**→**Cb**), T_c decreases because of the decrease in the absolute value of J_{MnNb} (from –15.1 to –10.4 cm^{-1}). The number of nearest neighbours remains the same (eight and four for the Nb and Mn centres, respectively) and does not contribute to the change in T_c. The decrease of the absolute value of J_{MnNb} is most likely caused by the increase of the coordination number of Mn^{II} centres back to six [the empty sites in the coordination spheres of Mn^{II} in **Ca** are taken up by water molecules].

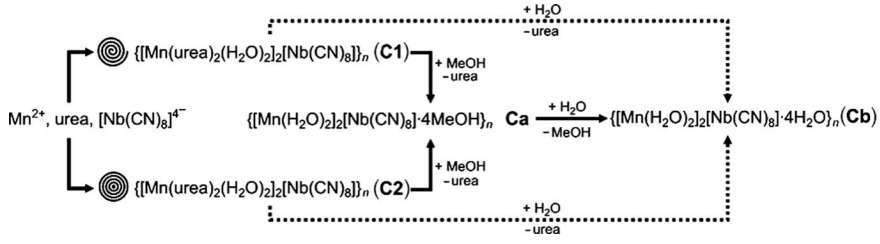

Scheme 1. The reactivity of the $\{[Mn^{II}(urea)_2(H_2O)]_2[Nb^{IV}(CN)_8]\}_n$ system.

It is remarkable that the values of J_{MnNb} for **C** and **Cb** are almost equal, while the critical temperature of **Cb** is higher by about 5 K. The shift of T_c in this case can easily be explained in terms of increased connectivity type (number of nearest neighbours) for **Cb** in comparison to **C** (8/4 and 6/3, respectively).

3.4. Acentric Networks and Chiral Networks

The absence of an inversion centre symmetry element in the crystal lattice is a requirement for observation of a series of interesting properties: second-order nonlinear optical (NLO) effects resulting, for example, in second harmonic generation (SHG), piezoelectricity, pyroelectricity, ferroelectricity, or chirality. These functions may be obtained, in the most straightforward approach, by the deliberate use of noncentrosymmetric building blocks having such features as high dipolar moment, high polarizability or, in the last case, a chiral component. An alternative way towards functional acentric and chiral networks may be the spontaneous resolution from building blocks, which do not bear the respective properties. The bulk functions appear in case of the space symmetry groups without an inversion centre and with some special symmetry elements such as the screw-axis.[1f]

Table 6 collects octacyanometallate-based acentric networks, chiral networks, and other networks containing chiral motives like tris-chelated complexes and helical chains or strands. The most important structural and physical features are included. The majority of those networks were obtained by spontaneous resolution. Multifunctional networks with magnetic ordering below T_c are of particular interest, as the simultaneous presence of these properties may lead to the observation of second-order phenomena: the strong magnetochiral dichroism[6e] and MSHG (magnetization-induced SHG).[6f] Only the second effect was observed for two octacyanometallate-based magnets;[23c,139] however, one chiral magnet $[W(CN)_8]_4[Cu(S\text{-}pn)H_2O]_4[Cu(S\text{-}pn)]_2{\cdot}2.5H_2O$ was characterized and compared to its racemic congener.[111] The α-$\{[Mn^{II}(urea)_2(H_2O)]_2[Nb^{IV}(CN)_8]\}_n$ polymorph presented in the previous section is an acentric and chiral magnet of crossed-ladder-type topology having a T_c of 43 K (Figure 12b).[23] Within the frame of the $P4_1$ space group, the magnetic space group was proposed to be $P2_1$. The polarization axis running along the *c* direction is orthogonal to the easy magnetization axes *a* and *b*. Along 4_1 screw axes collinear with the *c* axis, helical motives of corner sharing squares, Mn_2Nb_2, are observed. The compound revealed constant intensity of SH light above the magnetic ordering temperature. In the magnetic field of 500 G applied along the *a* direction, the SH signal below the ordering temperature started to increase sharply to reach at $T = 10$ K, a value four times higher than that measured above the T_c. The chirality could not be confirmed because of the twinning of the monocrystal. It is worth mentioning that subtle changes in the synthetic procedure, that is, in the concentration or ionic strength, may result in the appearance of polymorphs or very closely related species, which would not exhibit the desired properties (SHG, charge transfer etc.) because of the absence of favourable structural conditions.[130,22a,138]

Table 6. Overview of noncentrosymmetric networks and related properties of octacyanometallate-based compounds.

SHG (MSHG) function

Compound, T_c	Space group (magn. space gr.)[a]	Polarization axis (easy magn. axis, T_c)[a]	Special symmetry features	SHG intensity at r.t. [esu] (% vs. KDP), (MSHG vs. SHG)	Ref.
{MnpyzMo}	$P2_1$	*B*	$2_1 \parallel b$	6×10^{-11} (4%)	[137]
{MnpyzNb}, 48 K	$P2_1$ ($P2_1$)	*b* (*a*)	$2_1 \parallel b$	2×10^{-11} (1.3%), (×3)	[138,139]
{MnureaNb-α}, 43 K	$P4_1$ ($P2_1$)	*c* (*a*, *b*)	$4_1 \parallel c$	(×4)	[23c]
$CuNH_3Mo$	*Fdd*2	*c*	asymmetric distribution of bridging and terminal CN^- ligands	1.8×10^{-10} (12%)	[160]

Ferroelectric network

CuMo, amorphic ferroelectric, remnant electric polarization $P_r = 0.036$ μC·cm^{-2}, electric coercive field (E_c) of 5.5 kV cm^{-1}, the electric polarization is maintained by the structural local disorder of hydrogen bonding and the 3D CN network (due to freezing point for the fixation of hydrogen bonding at 150 K), polar group of $C_{\infty v}$ after application of an electric field.[161]

Chiral networks and chiral coordination motives

Network	Magnetic function	Space group	Chirality	T_c [K]	H_c [Oe]	M_{sat} [Nβ]	Ref.
CupnW	yes	$P2_1$	1S enantiomer	7.5	52	9.6	[111]
		$P2_1/c$	none (*rac*)	8.5	186	9.6	
NitrenMo	no	$P2_12_12_1$	racemic mixture of chiral triple-stranded chains	–	–	–	[84]
$[M(en)_3][M(en)_2W]$	no	$P2_12_12_1$	crystal with $[\Delta\text{-}M(en)_3]$ $[\Lambda\text{-}M(en)_3]$ cations grows selectively from the racemic mixtures	–	–	–	[31]

[a] Operating for magnetic networks.

3.5. Slow Magnetic Relaxation Processes in Low-Dimensional Systems

Low-dimensional coordination assemblies are of interest due to their potential ability to act as nanometric size single-domain magnetic objects called SMMs for discrete species and SCMs for 1D species. The key feature in the construction of such materials is the strong axial single-ion anisotropy resulting from nonzero orbital contribution to the total momentum, expressed by the negative parameter *D*. The intracluster interaction should stabilize a relatively high-spin ground state *S*. This may be provided by ions with a large number of ferromagnetically coupled unpaired electrons. These two contributions are to ensure a high energy barrier, U_{eff}, for transfer between $+S$ and $-S$ states and related blocking temperatures T_B. The 3d ions such as Mn^{III}, Mn^{IV}, Fe^{II}, Fe^{III}, Co^{II} and Ni^{II}, as well as highly anisotropic lanthanide ions such as Tb^{III}, Dy^{III} or Ho^{III} are of particular interest in this respect. To successfully obtain SMM/SCM compounds it is necessary to ensure that the intercluster/interchain interactions are much weaker relative to the barrier height U_{eff}. It occurs naturally for low-dimensional species and may be supported by locating the bulky organic ligands at the external part of the coordination skeleton. The most effective ones from the point of view of energy barrier and relaxation times were Mn^{III}, Mn^{IV} and Tb^{III} (the latter first of all in the case of phthalocyanine complexes).[7,8]

Several strategies were implemented to synthesize novel low-dimensional octacyanometallate-based compounds revealing some SMM- or SCM-like features (Table 7). Octacyanometallates themselves do not show significant internal anisotropy. However, possessing $S = 1/2$ they may serve as the bridging complexes in building high-spin species regardless of whether ferromagnetic (F) or antiferromagnetic (AF) interactions operate. Among the most dynamically studied complexes are high-spin pentadecanuclear clusters of the general formula $\{M'^{II}_9[M''^{V}(CN)_8]_6(solv)_{24}\}$ and $\{M'^{II}_9[M''^{V}(CN)_8]_6L_8(solv)_8\}$ (M′ = Ni, Co; M″ = Mo, W; solv = ROH, H_2O; L = bidentate heterocyclic chelating ligands) (Figure 3c).[60,63,66,67,69] The second class of compounds are trimetallic $\{M'Ln^{III}L\}[M''(CN)_8]$ (M′ = Cu^{II},

Table 7. Overview of parameters illustrating SMM-like and SCM-like features in octacyanometallate-based compounds.

Compound	S_{gr}, type of interactions,[a] coupling and magnetic anisotropy parameters	$[\chi''(T)]_{max}(f)$ above T = 2 K,[b] (χ''max/χ'max)[c]	$M(H/T)$	$\Delta T_p/T_p\Delta(\log\omega)$	τ_0 [s]	U_{eff} [cm^{-1}]	Hysteresis loop	Refs.
0D systems								
$Co^{II}_9W^{V}_6(MeOH)_{24}$	S = 21/2, AF	present (0.19)[d]	Yes	0.13	7.39×10^{-11}	19.3	n.r.	[69]
$Co^{II}_9Mo^{II}_6(MeOH)_{24}$	–	onset	–	–	–	–	n.r.	[63]
$Co^{II}_9M^{V}_5Re^{V}(MeOH)_{24}$								
$Ni^{II}_9W^{V}_6(2,2'\text{-bpy})_8$	S = 12, F	present (0.015)	Yes	0.13	1.5×10^{-13}	33.0	n.r.	[67]
$Ni^{II}_9W^{II}_6(btz)_8$	S = 12, F, D = 0.054 cm^{-1}	absent	Yes	–	–	–	n.r.	[66]
$Ni^{II}_3M^{V}_2(tmphen)_6$	S = 4, F, J = 10 cm^{-1} D = –0.24 cm^{-1}	onset	Yes	–	–	–	no	[60]
$Ni^{II}_9W^{V}_6(tmphen)_6$	S = 12, F, J = 12 cm^{-1} D = –0.04 cm^{-1}	onset	Yes	–	–	3.9[e]	yes[f]	[60]
$\{Ni^{II}(H_2O)L^{5}Tb^{III}(dmf)_{2.5}(H_2O)_{1.5}\}$ $\{W(CN)_8\}\cdot H_2O\cdot0.5dmf$	–	present (0.42)	n.r.	n.r.	4.5×10^{-7}	10.6	n.r.	[41]
$\{Ni^{II}(dmf)L^{5}Tb^{III}(dmf)_4\}$ $\{W(CN)_8\}\cdot0.5dmf$	–	onset	n.r	–	–	–	n.r.	[41]
$\{Ni^{II}(H_2O)L^{5}Ln^{III}(H_2O)_{4.5}\}_2$ $[W^{V}(CN)_8]\cdot15H_2O$, Ln = Tb, Dy	–	onset	n.r.	–	–	–	n.r.	[48]
$[(Mo^{V}(CN)_8)_2(CuL^{11}Tb)_4][Mo(CN)_8]$ $\cdot19H_2O$	–	present[g]	n.r.	n.r.	2.12×10^{-6}	13.4	n.r.	[58]
1D systems								
$[\{(Cu^{II}L^{15})_2Dy^{III}\}\{Mo^{V}(CN)_8\}]$ $\cdot MeCN\cdot H_2O$	J_{CuMo} = 1.5, 5.2 cm^{-1}[h]	present (0.42)[i]	n.r.	0.3	1.28×10^{-7}	13.2	n.r.	[94]
$[Mn^{III}(Cl\text{-salen})]_2[M^{V}(CN)_8]$	AF	onset	n.r.	–	–	–	n.r.	[75]
$[\{(H_2O)Fe(L^{14})\}\{M^{IV}(CN)_8\}\{Fe(L^{14})\}]_\infty$	J = –20 cm^{-1} D_{Fe} = –17 cm^{-1}	present (0.20)[j]	Yes	–	4.6×10^{-11}	51.4	yes[k]	[74]

[a] F = ferromagnetic, AF = antiferromagnetic. [b] Onset of the dependence of $\chi''(T)$ signal are observed, with the maxima expected below 2 K. [c] Measured at frequency f = 1 kHz. [d] The maxima in $\chi''(T)$ for some frequencies were acquired by the extrapolation of experimental results with Lorenz functions. [e] Calculated by using the $S_z^2|D|$ formula. [f] Measured at a sweep rate 0.017 T s^{-1}; coercivity that depends strongly on temperature and sweep rate is observed. [g] The frequency-dependent signal partially overlaps with another low-temperature magnetic feature (not interpreted by the authors). [h] Obtained from DFT calculations. [i] Cole–Cole plot indicates multiple relaxation processes. [j] Cole–Cole plot indicates broad distribution of relaxation times. [k] Smooth hysteresis is observed at 1 K, while at 0.38 K abrupt reversals occur with field sweeping.

Ni^{II}; Ln = lanthanide; L = tetradentate Schiff base ligands; M′′ = Mo^{V}, W^{V}), in which planar bimetallic adducts $\{M'Ln^{III}L\}$ are typically connected by $[M(CN)_8]^{3-}$ bridges into open-chain or closed-ring oligomers and 1D chains (Figure 4k).[41,48,58,74,79] In most of these compounds, the frequency-dependent $\chi''(T)$ curves indicate clearly the presence of a magnetic relaxation processes; however, the respective maxima fall in the majority of cases very close to or just below the measurement limit of 1.8 K in the typical SQUID apparatus. This fact strongly limits the accuracy of calculation of τ_0 and U_{eff} or even makes their estimation impossible. The relatively broad shape of $\chi''(T)$ signals indicates the large distribution of relaxation times. A $\chi''(T)_{max}/\chi'(T)_{max}$ ratio that does not exceed 0.2, a value significantly lower than that for typical SMMs, indicates the impure character of SMM relaxation, possibly with some spin-glass contribution. The reduced magnetization $M(H/T)$ reveals noncollinearity in different magnetic fields, which allowed to estimate the magnetic anisotropy parameters. It is worth noting, however, that bridging of $\{M'Ln^{III}L\}$ with $[M(CN)_8]^{3-}$ enhances the overall anisotropy of the system. The magnetic hysteresis loop at low temperature, which is believed to be the most indicative probe for SMM or SCM species, was reported only in two cases: for the $\{Ni^{II}[Ni^{II}(tmphen)(CH_3OH)]_6[Ni(H_2O)_3]_2[W^{V}(CN)_8]_6\}$[60] cluster with two opposite terminal Ni moieties not capped by bidentate ligands and for the $[\{Fe^{II}L\}\{Nb^{IV}(CN)\}]$[74] (L = pentadentate macrocycle) chain, where the source of anisotropy was the unusual pentagonal bipyramidal 7-coordination of Fe^{II} centres. Cascade-like hysteresis at 300 mK was observed in the latter case.

3.6. Spin Crossover

Only one example of octacyanometallate-based spin-crossover systems has been reported to date for 3D network $(HS)Fe_2[Nb(CN)_8]\cdot(3\text{-py}CH_3OH)\cdot 4.6H_2O$, in which 3-py$CH_3OH$ is (3-pyridyl)methanol. $[Nb(CN)_8]^{4-}$ of dodecahedral geometry forms four equatorial CN^- bridges, while the pseudo-octahedral Fe^{II} centre joins two CN^- bridges in axial positions and four 3-pyCH_3OH in equatorial positions. The reversible spin-crossover transition involving only half of the Fe^{II} sites goes gradually from $[(HS)Fe^{II}]_2Nb$ at 298 K to $(LS)Fe^{II}(HS)Fe^{II}Nb^{IV}$ at about 150 K. The low-temperature phase orders at a T_c of 12 K and reveals a magnetic hysteresis loop with a H_c of approximately 1000 Oe.[162]

3.7. Luminescence

Lanthanide-centred luminescence was observed in square grid 2D networks $Ln^{III}(H_2O)_5[M^{V}(CN)_8]$, where Ln = Eu, Tb and M = Mo, W. The excitation spectra monitored with the $^5D_4\rightarrow{}^7F_5$ transition (544 nm) for Tb-containing compounds and with $^5D_0\rightarrow{}^7F_2$ (618 nm) transition for Eu-containing compounds revealed full sets of bands characteristic for the respective intra 4f-transition-based excitation paths $^7F_6\rightarrow{}^5D_{0,1,3}$, $^5G_{4-6}$, $^5L_{10}$ (310–390 nm) for Tb^{III} and $^7F_0\rightarrow{}^5D_{4,2,1}$, $^5G_{2-4}$, $^5L_6$ (350–540 nm) for Eu^{III}. These excitation spectra also revealed broad bands below 310 nm, best pronounced for the TbW compound, which ware assigned to the domination of alternative excitation pathways exploiting the LMCT transitions. The emission spectra also showed the typical band sets for the incorporated lanthanides: $^5D_4\rightarrow{}^7F_{6-2}$ for Tb^{III} and $^5D_0\rightarrow{}^7F_{0-4}$ for Eu^{III}. The lifetimes of the respective excited states were calculated to be of order of milliseconds. The Tb-containing networks additionally revealed long-range magnetic ordering at low temperatures.[102,103]

4. Outlook and Perspectives

This Microreview shows the potential of octacyanometallates in the research on molecular materials: the ability to form the original topologies and the perspectives to obtain physical characteristic desired for switchable materials. Several research pathways may be pointed out to further development.

The stereochemical and electrochemical nonrigidity of $[M(CN)_8]^{n-}$ allowed their incorporation in networks of the magnetic state tuneable by the physical stimuli. Among the MMCT systems, $Cu^{II}Mo^{IV}$ and $Co^{II}W^{V}$ compounds were exploited to some point, while the similar activity of Co^{II}-Mo^{V} systems are still unexplored. The relatively high redox potential of the Mo^{V}/Mo^{IV} pair may move the critical region of the $Mo^{IV}Co^{III} \leftrightarrows Mo^{V}Co^{II}$ equilibrium to the higher temperatures compared to that of the $W^{IV}Co^{III} \leftrightarrows W^{V}Co^{II}$ equilibrium.

In our last perspective article,[163] we pointed out the possible routes for increasing the T_c above the limit of 55 K observed for the reported Mn^{II}-, Fe^{II}-, Co^{II}-, and Cu^{II}-octacyanometallate networks. It was shown for various cyanide-bridged networks that the desolvation leading to the decreased coordination number of the M'^{II} moiety may significantly increase the T_c. In some particular cases we can tune T_c, by influencing indirectly the strength of the magnetic interaction by the use of decorating organic ligands in the coordination sphere of M'^{II}. Finally, the magnetostructural correlation found for the $\{[M'^{II}(pyrazole)_4]_2[Nb^{IV}(CN)_8]\cdot 4H_2O\}_n$ series suggests that the use of V(II), V(III), Cr(II) or Cr^{III} complexes may increase the strength of the M′–M magnetic interaction, which results in a higher T_c. This is in good agreement with a T_c of 138 K reported very recently for $V^{II}V^{III}[Nb^{IV}(CN)_8]$.[164] We believe that the combination of the above strategies will make it possible to exceed this value in the nearest future; the possibility of approaching closely the room-temperature limit is not excluded. Multifunctional networks combining magnetic ordering with acentric or chiral networks could possibly be obtained. Organization of discrete cyanide-bridged species by organic linkers can lead to the construction of active porous magnetic networks.

As far as SMM and SCM systems are concerned, the application of octacyanometallates made it possible to gain or improve magnetic relaxation characteristics relative to

those of the precursors. However, as they only approach (qualitatively and quantitatively) those of classical SMM and SCM systems based on o Mn^{III} and Mn^{IV}, novel strategies are required. In our opinion, further improvement could be, in an optimistic scenario, possible by (1) tuning of the coordination sphere of anisotropic centres, (2) their distribution in the coordination skeleton and (3) intermolecular arrangement towards minimizing intermolecular interactions, which could be done with the tools offered by supramolecular chemistry.

Other functionalities of interest, Fe-centred SCO transition and lanthanide-centred luminescence, have been very scarcely represented in octacyanometallate-based solid-state systems until now. We have shown that the *trans*-[Fe(μ-$NC)_4(H_2O)_2$] nodes in closely packed magnetic Fe_2Nb networks with T_c = 43 K retained HS configuration in the temperature range 2–300 K. The SCO effect was observed for the *trans*-[Fe(μ-$NC)_2$(3-py$CH_3OH)_4$] moiety in bimetallic Fe^{II}_2(3-pyCH_3OH)Nb^{IV}, yet the decrease of cyanide-bridged connectivity and spin crossover itself resulted in significant lowering of T_c below the range where SCO normally occurs. It is, however, possible that irradiating the low-spin phase, (LS)Fe^{II}(HS)$Fe^{II}Nb^{IV}$, may cause a LIESST effect leading to the novel metastable state (HS)$Fe^{II}_2Nb^{IV}$ with full sets of Fe^{II} centres.

Leaving the first decade of the XXI century behind, we have gathered the solid experience and knowledge of the potential carried by octacyanometallates with respect to the search for functional materials. The collected examples of synthetic strategies would allow for more judicious and precise choice of the building blocks in the design of novel functional systems. The advanced and elaborate techniques including coupling of the measurement of physical properties with the external stimuli applied in situ or the use of synchrotron radiation techniques become a standard in the characterization of different states in switchable materials. The research in this field continues, and the new original reports are expected to realize the ideas being formulated at the crossroads of crystal engineering and material science.

Acknowledgments

This study has been partially supported by the European Commission (EC), within NoE project MAGMANet, contract no. NMP3-CT-2005-515767, by the Polish Ministry of Science and Higher Education within research projects 1535/B/H03/2009/36, 0538/B/H03/2008/35 3327/B/H03/2009/37 and 0087-B-H03-2008-34, and by the European Union (EU), within the Integrated Regional Operational Programme, Priority II: Strengthening the Human Resources Development in Regions, Project Małopolskie Stypendium Doktoranckie (IROP2004-2006).

[1] a) C. Janiak, *Dalton Trans.* **2003**, 2781–2804; b) S. Kitagawa, R. Kitaura, S. Noro, *Angew. Chem.* **2004**, *116*, 2388; *Angew. Chem. Int. Ed.* **2004**, *43*, 2334–2375; c) P. S. Suh, Y. E. Cheon, E. Y. Lee, *Coord. Chem. Rev.* **2008**, *252*, 1007–1026; d) M. Fujita, K. Umemoto, M. Yoshizawa, N. Fujita, T. Kusukawa, K. Biradha, *Chem. Commun.* **2001**, 509–518; e) V. Maurizot, M. Yoshizawa, M. Kawano, M. Fujita, *Dalton Trans.* **2006**, 2750–2756; f) S. R. Batten, S. M. Neville, D. Turner, *Coordination Polymers: Design, Analysis and Applications*, **2009**, The Royal Society of Chemistry, Cambridge, UK, ch. 11.

[2] a) O. Sato, J. Tao, Y. Z. Zhang, *Angew. Chem.* **2007**, *119*, 2200; *Angew. Chem. Int. Ed.* **2007**, *46*, 2152–2187; b) M. Ohba, K. Yoneda, G. Augusti, M. C. Muñoz, A. B. Gaspar, J. A. Real, M. Yamasaki, H. Ando, Y. Nakao, S. Sasaki, S. Kitagawa, *Angew. Chem.* **2009**, *121*, 4861; *Angew. Chem. Int. Ed.* **2009**, *48*, 4767–4771; c) G. Agustí, A. Cobo, A. B. Gaspar, G. Molnar, N. O. Moussa, P. Szilágyi, V. Pálfi, C. Vieu, M. C. Muñoz, J. A. Real, A. Bousseksou, *Chem. Mater.* **2008**, *20*, 6721–6732; d) S. Bonhommeau, G. Molnar, A. Galet, A. Zwick, J. A. Real, J. J. McGarvey, A. Bousseksou, *Angew. Chem.* **2005**, *117*, 4137; *Angew. Chem. Int. Ed.* **2005**, *44*, 4069–4073; e) G. Molnar, V. Niel, J. A. Real, L. Dubrovinsky, A. Bousseksou, J. J. McGarvey, *J. Phys. Chem. B* **2003**, *107*, 3149–3155; f) S. Bonhommeau, G. Molnar, M. Gorain, K. Boukheddaden, A. Bousseksou, *Phys. Rev. B* **2006**, *74*, 064424; g) I. Boldog, A. B. Gaspar, V. Martinez, P. Pardo-Ibañez, V. Ksenofontov, A. Bhattacharjee, P. Gütlich, J. A. Real, *Angew. Chem.* **2008**, *120*, 6533; *Angew. Chem. Int. Ed.* **2008**, *47*, 6433–6437; h) P. Gamez, J. Sanchez Costa, M. Quesada, G. Aromi, *Dalton Trans.* **2009**, 7845–7853.

[3] a) M. Eddaoudi, J. Kim, N. Rosi, D. Vodak, J. Watcher, M. O'Keeffe, O. M. Yaghi, *Science* **2002**, *295*, 496–472; b) J. J. Perry IV, J. A. Perman, M. J. Zaworotko, *Chem. Soc. Rev.* **2009**, *38*, 1400–1417; c) D. J. Tranchemontagne, J. L. Mendoza-Cortés, M. O'Keeffe, O. M. Yaghi, *Chem. Soc. Rev.* **2009**, *38*, 1257–1283; d) R. Robson, *Dalton Trans.* **2008**, 5113–5131.

[4] a) G. Férey, *Dalton Trans.* **2009**, 4400–4415; b) F. Millange, C. Serre, N. Guillou, G. Férey, R. I. Walton, *Angew. Chem.* **2008**, *120*, 4168; *Angew. Chem. Int. Ed.* **2008**, *47*, 4100–4105; c) P. L. Llewellyn, G. Maurin, T. Devic, S. Loera-Serna, N. Rosenbach, C. Serre, S. Bourrelly, P. Horcajada, Y. Filinchuk, G. Férey, *J. Am. Chem. Soc.* **2008**, *130*, 12808–12814; d) Y. Liu, J. H. Her, A. Dailly, A. J. Ramirez-Cuesta, D. A. Neumann, C. M. Brown, *J. Am. Chem. Soc.* **2008**, *130*, 11813–11818.

[5] a) Y. Wei, Y. Yu, K. Wu, *Cryst. Growth Des.* **2007**, *7*, 2262–2264; b) Y.-M. Xie, Q.-S. Zhang, Z.-G. Zhao, X.-Y. Wu, S.-C. Chen, C.-Z. Lu, *Inorg. Chem.* **2008**, *47*, 8086–8090.

[6] a) D. Bradshaw, T. J. Prior, E. J. Cussen, J. B. Claridge, M. J. Rosseinsky, *J. Am. Chem. Soc.* **2004**, *126*, 6106–6114; b) J. Heo, Y.-M. Jeon, C. A. Mirkin, *J. Am. Chem. Soc.* **2007**, *129*, 7712–7713; c) E. Coronado, J. R. Galan-Mascaros, C. J. Gomez-Garcia, E. Martinez-Ferrero, M. Almeida, J. C. Waerenborgh, *Eur. J. Inorg. Chem.* **2005**, 2064–2070; d) O. Sereda, J. Ribas, H. Stoeckli-Evans, *Inorg. Chem.* **2008**, *47*, 5107–5113; e) C. Train, R. Gheorghe, V. Krstic, L.-M. Chamoreau, N. S. Ovanesyan, G. L. J. A. Rikken, M. Gruselle, M. Verdaguer, *Nat. Mater.* **2008**, *7*, 729–734; f) C. Train, T. Nuida, R. Gheorghe, M. Gruselle, S. Ohkoshi, *J. Am. Chem. Soc.* **2009**, *131*, 16838–16843.

[7] a) D. Gatteschi, R. Sessoli, A. Cornia, "Magnetism from the Molecular to the Nanoscale" in *Comprehensive Coordination Chemistry II* (Eds.: J. A. McCleverty, T. J. Meyer), *Vol. 7: From the Molecular to the Nanoscale: Synthesis, Structure, and Properties* (Eds.: M. Fujita, A. Powell, C. Creutz), **2005**, Elsevier, Amsterdam, ch. 7.13, p. 779–813; b) D. Gatteschi, R. Sessoli, J. Villain, *Molecular Nanomagnets*, Oxford University Press, New York, **2006**; c) T. C. Stamatatos, D. Foguet-Albiol, S. C. Lee, C. C. Stoumpos, C. P. Raptopoulou, A. Terzis, W. Wernsdorfer, S. O. Hill, S. P. Perlepes, G. Christou, *J. Am. Chem. Soc.* **2007**, *129*, 9484–9499; d) A. J. Tasiopoulos, S. P. Perlepes, *Dalton Trans.* **2008**, 5537–5555; e) A.-R. Tomsa, J.-M. Lillo, Y. Li, L.-M. Chamoreau, K. Boubekeur, F. Farias, M. A. Novak, E. Cremades, E. Ruiz, A. Proust, M. Verdaguer, P. Gouzerh, *Chem. Commun.* **2010**, *46*, 5106–5108; f) M. Murrie, *Chem. Soc. Rev.* **2010**, *39*, 1986–1995.

[8] a) H. Miyasaka, R. Clérac, *Bull. Chem. Soc. Jpn.* **2005**, *78*, 1725–1748; b) H. Miyasaka, M. Yamashita, *Dalton Trans.*

2007, 399–406; c) H. Miyasaka, M. Julve, M. Yamashita, R. Clérac, *Inorg. Chem.* **2009**, *48*, 3420–3437; d) H. L. Sun, Z. M. Wang, S. Gao, *Coord. Chem. Rev.* **2010**, *254*, 1081–1100.

[9] J. A. Real, A. B. Gaspar, M. C. Munoz, *Dalton Trans.* **2005**, 2062–2079.

[10] a) M. Verdaguer, A. Bleuzen, V. Marvaud, J. Vaisserman, M. Seuleiman, C. Desplanches, C. Train, R. Garde, G. Gelly, C. Lomenech, I. Rosenman, P. Veillet, C. Cartier, F. Villain, *Coord. Chem. Rev.* **1999**, *190–192*, 1023–1047; b) S. Tanase, F. Tuna, P. Guionneau, T. Maris, G. Rombaut, C. Mathoniere, M. Andruh, O. Kahn, J.-P. Sutter, *Inorg. Chem.* **2003**, *42*, 1625–1631; c) Y. Sato, S. Ohkoshi, K. Arai, M. Tozawa, K. Hashimoto, *J. Am. Chem. Soc.* **2003**, *125*, 14590–14595; d) M. D. Harvey, T. D. Crawford, G. T. Yee, *Inorg. Chem.* **2008**, *47*, 5649–5655; e) M. Ohba, W. Kaneko, S. Kitagawa, T. Maeda, M. Mito, *J. Am. Chem. Soc.* **2008**, *130*, 4475–4484; f) N. Motokawa, H. Miyasaka, M. Yamashita, K. R. Dunbar, *Angew. Chem.* **2008**, *120*, 7874; *Angew. Chem. Int. Ed.* **2008**, *47*, 7760–7763; g) C. Mathoniere, C. J. Nuttal, S. G. Carling, P. Day, *Inorg. Chem.* **1996**, *35*, 1201–1206; h) D. Armentano, G. De Munno, F. Lloret, A. V. Palii, M. Julve, *Inorg. Chem.* **2002**, *41*, 2007–2013; i) D. Armentano, G. De Munno, T. F. Mastropietro, D. M. Proserpio, M. Julve, F. Lloret, *Inorg. Chem.* **2004**, *43*, 5177–5179; j) B.-Q. Ma, H.-L. Sun, S. Gao, G. Su, *Chem. Mater.* **2001**, *13*, 1946–1948; k) X. Hao, Y. Wei, S. Zhang, *Chem. Commun.* **2000**, 2271–2272; l) O. Kahn, J. Larionova, J. V. Yakhmi, *Chem. Eur. J.* **1999**, *5*, 3443–3449; m) J. L. Manson, C. R. Kmety, A. J. Epstein, J. S. Miller, *Inorg. Chem.* **1999**, *38*, 2552–2553; n) K. Barthelet, J. Marrot, D. Riou, G. Férey, *Angew. Chem.* **2002**, *114*, 291; *Angew. Chem. Int. Ed.* **2002**, *41*, 281–284.

[11] a) K. R. Dunbar, R. A. Heintz, *Progr. Inorg. Chem.* (Ed.: K. D. Karlin), John Wiley & Sons, Hoboken, NJ, **1997**, vol. 45, pp. 283–391; b) M. Ohba, H. Okawa, *Coord. Chem. Rev.* **2000**, *198*, 313–328; c) J. Černák, M. Orendáč, I. Potočňák, J. Chomič, A. Orendačová, J. Skorupa, A. Feher, *Coord. Chem. Rev.* **2002**, *224*, 51–66; d) C. J. Shorrock, H. Jong, R. J. Batchelor, D. B. Leznoff, *Inorg. Chem.* **2003**, *42*, 3917–3924; e) D. E. Freedman, D. M. Jenkins, A. T. Iavarone, J. R. Long, *J. Am. Chem. Soc.* **2008**, *130*, 2884–2885; f) X.-Y. Wang, A. V. Prosvirin, K. R. Dunbar, *Angew. Chem. Int. Ed.* **2010**, *49*, 5081–5084; g) M. Shatruk, C. Avendano, K. R. Dunbar, *Progr. Inorg. Chem.* (Ed.: K. D. Karlin), John Wiley & Sons, Hoboken, NJ, **2009**, vol. 56, pp. 155–334.

[12] a) B. Sieklucka, R. Podgajny, P. Przychodzeń, T. Korzeniak, *Coord. Chem. Rev.* **2005**, *249*, 2203–2221; b) P. Przychodzeń, T. Korzeniak, R. Podgajny, B. Sieklucka, *Coord. Chem. Rev.* **2006**, *250*, 2234–2260.

[13] B. Sieklucka, J. Szklarzewicz, T. J. Kemp, W. Errington, *Inorg. Chem.* **2000**, *39*, 5156–5168.

[14] a) Z. J. Zhong, H. Seino, M. Gross, Y. Mizobe, M. Hidai, A. Fujishima, S. Ohkoshi, K. Hashimoto, *J. Am. Chem. Soc.* **2000**, *122*, 2952–2953; b) F. Bonadio, J. Larionova, M. Gross, M. Biner, H. Stoeckli-Evans, S. Decurtins, M. Pilkington, *Inorg. Synth* (Ed.: J. R. Shapley), John Wiley & Sons, Inc., Hoboken, NJ, **2004**, vol. 34, pp. 156–160.

[15] a) J. Larionova, M. Gross, M. Pilkington, H. Andres, H. Stoeckli-Evans, H. U. Güdel, S. Decurtins, *Angew. Chem.* **2000**, *112*, 1667; *Angew. Chem. Int. Ed.* **2000**, *39*, 1605–1609; b) E. Ruiz, G. Rajaraman, S. Alvarez, B. Gillon, J. Stride, R. Clérac, J. Larionova, S. Decurtins, *Angew. Chem.* **2005**, *117*, 2771; *Angew. Chem. Int. Ed.* **2005**, *44*, 2711–2715; c) Y. Q. Zhang, C. L. Luo, *Dalton Trans.* **2008**, 4575–4584.

[16] Z.-J. Zhong, H. Seino, Y. Mizobe, M. Hidai, M. Verdaguer, S. Ohkoshi, K. Hashimoto, *Inorg. Chem.* **2000**, *39*, 5095–5101.

[17] M. Pilkington, S. Decurtins, *Chimia* **2000**, *54*, 593–601.

[18] a) R. Podgajny, T. Korzeniak, M. Bałanda, T. Wasiutyński, W. Errington, T. J. Kemp, N. W. Alcock, B. Sieklucka, *Chem. Commun.* **2002**, 1138–1139; b) T. Korzeniak, R. Podgajny, N. W. Alcock, K. Lewiński, M. Bałanda, T. Wasiutyński, B. Sieklucka, *Polyhedron* **2003**, *22*, 2183–2191; c) R. Podgajny, N. P. Chmel, M. Bałanda, P. Tracz, B. Gaweł, D. Zając, M. Sikora, C. Kapusta, W. Łasocha, T. Wasiutyński, B. Sieklucka, *J. Mater. Chem.* **2007**, *17*, 3308–3314.

[19] a) B. Sieklucka, T. Korzeniak, R. Podgajny, M. Bałanda, Y. Nakazawa, Y. Myiazaki, M. Sorai, T. Wasiutyński, *J. Magn. Magn. Mater.* **2004**, *272–276*, 1058–1059; b) M. Bałanda, T. Korzeniak, R. Pełka, R. Podgajny, M. Rams, B. Sieklucka, T. Wasiutyński, *Solid State Sci.* **2005**, *7*, 1113–1124; c) F. L. Pratt, P. M. Zieliński, M. Bałanda, R. Podgajny, T. Wasiutyński, B. Sieklucka, *J. Phys. Condens. Matter* **2007**, *19*, 456208; d) S. Kaneko, Y. Tsunobuchi, S. Sakurai, S. Ohkoshi, *Chem. Phys. Lett.* **2007**, *446*, 292–296; e) T. Hozumi, K. Hashimoto, S. Ohkoshi, *J. Am. Chem. Soc.* **2005**, *127*, 3864–3869; f) M. Bałanda, R. Pełka, T. Wasiutyński, M. Rams, Y. Nakazawa, Y. Miyazaki, M. Sorai, R. Podgajny, T. Korzeniak, B. Sieklucka, *Phys. Rev. B* **2008**, *78*, 174409; g) M. Czapla, R. Pełka, P. M. Zieliński, A. Budziak, M. Bałanda, M. Makarewicz, A. Pacyna, T. Wasiutyński, Y. Miyazaki, Y. Nakazawa, A. Inaba, M. Sorai, F. L. Pratt, R. Podgajny, T. Korzeniak, B. Sieklucka, *Phys. Rev. B* **2010**, *82*, 094446.

[20] T. Korzeniak, K. Stadnicka, M. Rams, B. Sieklucka, *Inorg. Chem.* **2004**, *43*, 4811–4813.

[21] C. Mathoniere, R. Podgajny, P. Guionneau, C. Labrugere, B. Sieklucka, *Chem. Mater.* **2005**, *17*, 442–449.

[22] D. Pinkowicz, R. Pełka, O. Drath, W. Nitek, M. Bałanda, A. M. Majcher, G. Ponetti, B. Sieklucka, *Inorg. Chem.* **2010**, *49*, 7565–7576.

[23] a) R. Podgajny, D. Pinkowicz, T. Korzeniak, W. Nitek, M. Rams, B. Sieklucka, *Inorg. Chem.* **2007**, *46*, 10416–10425; b) D. Pinkowicz, R. Podgajny, W. Nitek, M. Makarewicz, M. Czapla, M. Mihalik, M. Bałanda, B. Sieklucka, *Inorg. Chim. Acta* **2008**, *361*, 3957–3962; c) D. Pinkowicz, R. Podgajny, W. Nitek, M. Rams, A. M. Majcher, T. Nuida, S. Ohkoshi, B. Sieklucka, *Chem. Mater.* **2010**, DOI: 10.1021/cm102388q.

[24] B. Nowicka, M. Rams, K. Stadnicka, B. Sieklucka, *Inorg. Chem.* **2007**, *46*, 8123–8125.

[25] D. Pinkowicz, R. Podgajny, M. Bałanda, M. Makarewicz, B. Gaweł, W. Łasocha, B. Sieklucka, *Inorg. Chem.* **2008**, *47*, 9745–9747.

[26] a) R. Podgajny, W. Nitek, M. Rams, B. Sieklucka, *Cryst. Growth Des.* **2008**, *8*, 3817–3821; b) R. Podgajny, S. Chorąży, W. Nitek, M. Rams, M. Bałanda, B. Sieklucka, *Cryst. Growth Des.* **2010**, *10*, 4693–4696.

[27] M. J. Zaworotko, *Chem. Commun.* **2001**, 1–9.

[28] A. K. Cheetham, C. N. R. Rao, R. K. Feller, *Chem. Commun.* **2006**, 4780–4795.

[29] J. Qu, W. Gu, X. Liu, *J. Coord. Chem.* **2008**, *61*, 1782–1787.

[30] P. Przychodzeń, M. Rams, C. Guyard-Duhayon, B. Sieklucka, *Inorg. Chem. Commun.* **2005**, *8*, 350–354.

[31] J. R. Withers, C. Ruschmann, P. Bojang, S. Parkin, S. Holmes, *Inorg. Chem.* **2005**, *44*, 352–358.

[32] P. Przychodzeń, R. Pełka, K. Lewiński, J. Supel, M. Rams, K. Tomala, B. Sieklucka, *Inorg. Chem.* **2007**, *46*, 8924–8938.

[33] R. Podgajny, Y. Dromzée, K. Kruczała, B. Sieklucka, *Polyhedron* **2001**, *20*, 685–694.

[34] D. Visinescu, C. Desplanches, I. Imaz, V. Bahers, R. Pradhan, F. A. Villamena, P. Guionneau, J.-P. Sutter, *J. Am. Chem. Soc.* **2006**, *128*, 10202–10212.

[35] S.-Z. Zhan, J.-G. Wang, B. Long, H.-X. Shu, W.-Y. Yan, X.-J. Feng, *J. Coord. Chem.* **2008**, *61*, 1399–1405.

[36] U. Mukhopadhyay, I. Bernal, *Cryst. Growth Des.* **2005**, *5*, 1687–1689.

[37] G. Rombaut, M. Verelst, S. Golhen, L. Ouahab, C. Mathoniere, O. Kahn, *Inorg. Chem.* **2001**, *40*, 1151–1159.

[38] C. Mathoniere, H. Kobayashi, R. Le Bris, A. Kaïba, I. Bord, *C. R. Chim.* **2008**, *11*, 665–672.

[39] H. H. Ko, J. H. Lim, H. S. Yoo, J. S. Kang, H. C. Kim, E. K. Koh, C. S. Hong, *Dalton Trans.* **2007**, 2070–2076.

[40] S.-F. Si, X. Liu, D.-Z. Liao, S.-P. Yan, Z.-H. Jiang, P. Cheng, *J. Coord. Chem.* **2003**, *56*, 337–341.
[41] J.-P. Sutter, S. Dhers, R. Rajamani, S. Ramasesha, J.-P. Costes, C. Duhayon, L. Vendier, *Inorg. Chem.* **2009**, *48*, 5820–5828.
[42] T. Korzeniak, C. Desplanches, R. Podgajny, C. Giménez-Saiz, K. Stadnicka, M. Rams, B. Sieklucka, *Inorg. Chem.* **2009**, *48*, 2865–2872.
[43] H.-Z. Kou, B. C. Zhou, S.-F. Si, R.-J. Wang, *Eur. J. Inorg. Chem.* **2004**, 401–408.
[44] P. Przychodzeń, K. Lewiński, M. Bałanda, R. Pełka, M. Rams, T. Wasiutyński, C. G. Duhayon, B. Sieklucka, *Inorg. Chem.* **2004**, *43*, 2967–2974.
[45] M. Kozieł, R. Pełka, M. Rams, W. Nitek, B. Sieklucka, *Inorg. Chem.* **2010**, *49*, 4268–4277.
[46] R. Podgajny, C. Desplanches, B. Sieklucka, R. Sessoli, V. Villar, C. Paulsen, W. Wernsdorfer, Y. Dromzee, M. Verdaguer, *Inorg. Chem.* **2002**, *41*, 1323–1327.
[47] J.-P. Sutter, S. Dhers, J.-P. Costes, C. Duhayon, *C. R. Chim.* **2008**, *11*, 1200–1206.
[48] S. Dhers, S. Sahoo, J.-P. Costes, C. Duhayon, S. Ramasesha, J.-P. Sutter, *CrystEngComm* **2009**, *11*, 2078–2083.
[49] J. P. Lopez, F. W. Heinemann, A. Grohmann, *Z. Anorg. Allg. Chem.* **2003**, *629*, 2449–2457.
[50] C. Maxim, C. Mathoniere, M. Andruh, *Dalton Trans.* **2009**, 7805–7810.
[51] J. M. Herrera, V. Marvaud, M. Verdaguer, J. Marrot, M. Kalisz, C. Mathoniere, *Angew. Chem.* **2004**, *116*, 5584; *Angew. Chem. Int. Ed.* **2004**, *43*, 5468–5471.
[52] T. S. Venkatakrishnan, C. Desplanches, R. Rajamani, P. Guionneau, L. Ducasse, S. Ramasesha, J.-P. Sutter, *Inorg. Chem.* **2008**, *47*, 4854–4860.
[53] Z.-X. Wang, X.-L. Li, T.-W. Wang, Y.-Z. Li, S. Ohkoshi, Y. Song, X.-Z. You, *Inorg. Chem.* **2007**, *46*, 10990–10995.
[54] H. Zhao, M. Shatruk, A. V. Prosvirin, K. R. Dunbar, *Chem. Eur. J.* **2007**, *13*, 6573–6589.
[55] J. Wang, Y.-L. Xu, H.-B. Zhou, H.-S. Wang, X.-J. Song, Y. Song, X.-Z. You, *Dalton Trans.* **2010**, *39*, 3489–3494.
[56] R. Podgajny, T. Korzeniak, P. Przychodzeń, C. Giménez-Saiz, M. Rams, M. Kwaśniak, B. Sieklucka, *Eur. J. Inorg. Chem.* **2010**, 4166–4174.
[57] R. Kania, K. Lewiński, B. Sieklucka, *Dalton Trans.* **2003**, 1033–1040.
[58] J. Long, L.-M. Chamoreau, V. Marvaud, *Dalton Trans.* **2010**, *39*, 2188–2190.
[59] T. S. Venkatakrishnan, R. Rajamani, S. Ramasesha, J.-P. Sutter, *Inorg. Chem.* **2007**, *46*, 9569–9574.
[60] M. G. Hilfiger, H. Zhao, A. Prosvirin, W. Wernsdorfer, K. R. Dunbar, *Dalton Trans.* **2009**, 5155–5163.
[61] X. Chen, P. Yang, S.-L. Ma, S. Ren, M.-Y. Tang, Y. Yang, Z.-J. Guo, L.-Z. Liu, *J. Struct. Chem.* **2009**, *50*, 495–499.
[62] T. S. Venkatakrishnan, I. Imaz, J.-P. Sutter, *Inorg. Chim. Acta* **2008**, *361*, 3710–3713.
[63] D. E. Freedman, M. V. Bennett, J. R. Long, *Dalton Trans.* **2006**, 2829–2834.
[64] S.-L. Ma, S. Ren, Y. Ma, D.-Z. Liao, S.-P. Yan, *Struct. Chem.* **2009**, *20*, 161–167.
[65] F. Bonadio, M. Gross, H. Stoeckli-Evans, S. Decurtins, *Inorg. Chem.* **2002**, *41*, 5891–5896.
[66] J. H. Lim, H. S. Yoo, J. I. Kim, J. H. Yoon, N. Yang, E. K. Koh, J.-G. Park, C. S. Hong, *Eur. J. Inorg. Chem.* **2008**, 3428–3431.
[67] J. H. Lim, Y. H. Yoon, H. C. Kim, C. S. Hong, *Angew. Chem.* **2006**, *118*, 7584; *Angew. Chem. Int. Ed.* **2006**, *45*, 7424–7426.
[68] J. H. Lim, H. S. Yoo, Y. H. Yoon, E. K. Koh, H. C. Kim, C. S. Hong, *Polyhedron* **2008**, *27*, 299–303.
[69] Y. Song, P. Zhang, X.-M. Ren, X.-F. Shen, Y.-Z. Li, X.-Z. You, *J. Am. Chem. Soc.* **2005**, *127*, 3708–3709.
[70] M. Atanasov, P. Comba, Y. D. Lampeka, G. Linti, T. Malcherek, R. Miletich, A. I. Prikhod'ko, H. Pritzkow, *Chem. Eur. J.* **2006**, *12*, 737–748.
[71] R. Pradhan, C. Desplanches, P. Guionneau, J.-P. Sutter, *Inorg. Chem.* **2003**, *42*, 6607–6609.
[72] J. Wang, Z.-C. Zhang, H.-S. Wang, L.-C. Kang, H.-B. Zhou, Y. Song, X.-Z. You, *Inorg. Chem.* **2010**, *49*, 3101–3103.
[73] G. Rombaut, S. Golhen, L. Ouahab, C. Mathonière, O. Kahn, *J. Chem. Soc., Dalton Trans.* **2000**, 3609–3614.
[74] T. S. Venkatakrishnan, S. Sahoo, N. Brefuel, C. Duhayon, C. Paulsen, A.-L. Barra, S. Ramasesha, J.-P. Sutter, *J. Am. Chem. Soc.* **2010**, *132*, 6047–6056.
[75] H. S. Yoo, H. H. Ko, D. W. Ryu, J. W. Lee, J. H. Yoon, W. R. Lee, H. C. Kim, E. K. Koh, C. S. Hong, *Inorg. Chem.* **2009**, *48*, 5617–5619.
[76] S. Tanase, M. Evangelisti, L. Jos de Jongh, J. M. M. Smits, R. de Gelder, *Inorg. Chim. Acta* **2008**, *361*, 3548–3554.
[77] S. Tanase, L. Jos de Jongh, F. Prins, M. Evangelisti, *ChemPhysChem* **2008**, *9*, 1975–1978.
[78] F. Prins, E. Pasca, L. Jos de Jongh, H. Kooijman, A. L. Spek, S. Tanase, *Angew. Chem.* **2007**, *119*, 6193; *Angew. Chem. Int. Ed.* **2007**, *46*, 6081–6084.
[79] W. Kosaka, K. Hashimoto, S. Ohkoshi, *Bull. Chem. Soc. Jpn.* **2007**, *80*, 2350–2356.
[80] R. Pełka, M. Bałanda, P. Przychodzeń, K. Tomala, B. Sieklucka, T. Wasiutyński, *Phys. Status Solidi C* **2006**, *3*, 216–219.
[81] P. Przychodzeń, K. Lewiński, R. Pełka, M. Bałanda, K. Tomala, B. Sieklucka, *Dalton Trans.* **2006**, 625–628.
[82] J. R. Withers, C. Ruschman, S. Parkin, S. M. Holmes, *Polyhedron* **2005**, *24*, 1845–1854.
[83] S.-L. Ma, Y. Ma, S. Ren, S.-P. Yan, D.-Z. Liao, *Struct. Chem.* **2008**, *19*, 329–338.
[84] W. Zhang, Z.-Q. Wang, O. Sato, R.-G. Xiong, *Cryst. Growth Des.* **2009**, *9*, 2050–2053.
[85] R. Podgajny, R. Pełka, C. Desplanches, L. Ducasse, W. Nitek, T. Korzeniak, O. Stefańczyk, M. Rams, B. Sieklucka, M. Verdaguer, *Inorg. Chem.*, submitted.
[86] R. Podgajny, T. Korzeniak, K. Stadnicka, Y. Dromzée, N. W. Alcock, W. Errington, K. Kruczała, M. Bałanda, T. J. Kemp, M. Verdaguer, B. Sieklucka, *Dalton Trans.* **2003**, 3458–3468.
[87] Dong-feng Li, Song Gao, Li-min Zheng, Wen-xia Tang, *J. Chem. Soc., Dalton Trans.* **2002**, 2805–2806.
[88] D. Li, L. Zheng, Y. Zhang, J. Huang, S. Gao, W. Tang, *Inorg. Chem.* **2003**, *42*, 6123–6129.
[89] J. R. Withers, D. Li, J. Triplet, C. Ruschman, S. Parkin, G. Wang, G. T. Yee, S. M. Holmes, *Polyhedron* **2007**, *26*, 2353–2366.
[90] J. H. Lim, Y. S. You, H. S. Yoo, J. H. Yoon, J. I. Kim, E. K. Koh, C. S. Hong, *Inorg. Chem.* **2007**, *46*, 10578–10586.
[91] Y. S. You, D. Kim, Y. Do, S. J. Oh, C. S. Hong, *Inorg. Chem.* **2004**, *43*, 6899–6901.
[92] S.-L. Ma, S. Ren, *J. Inorg. Organomet. Polym.* **2009**, *19*, 382–388.
[93] J. Long, L.-M. Chamoreau, C. Mathoniere, V. Marvaud, *Inorg. Chem.* **2009**, *48*, 22–24.
[94] D. Visinescu, A. M. Madalan, M. Andruh, C. Duhayon, J.-P. Sutter, L. Ungur, W. Van den Heuvel, L. F. Chibotaru, *Chem. Eur. J.* **2009**, *15*, 11808–11814.
[95] J. H. Lim, J. S. Kang, H. C. Kim, E. K. Koh, C. S. Hong, *Inorg. Chem.* **2006**, *45*, 7821–7827.
[96] Y. S. You, J. H. Yoon, J. H. Lim, H. C. Kim, C. S. Hong, *Inorg. Chem.* **2005**, *44*, 7063–7069.
[97] A. H. Yuan, W. Y. Liu, H. Zhou, Y. Y. Chen, X. P. Shen, *J. Mol. Struct.* **2009**, *919*, 356–360.
[98] J. R. Withers, D. Li, J. Triplet, C. Ruschman, S. Parkin, G. Wang, G. T. Yee, S. M. Holmes, *Inorg. Chem.* **2006**, *45*, 4307–4309.
[99] Y. Arimoto, S. Ohkoshi, Z. J. Zhong, H. Seino, Y. Mizobe, K. Hashimoto, *J. Am. Chem. Soc.* **2003**, *125*, 9240–9241.
[100] D. Li, S. Gao, L. Zheng, K. Yuc, W. Tang, *New J. Chem.* **2002**, *26*, 1190–1195.
[101] T. Hozumi, S. Ohkoshi, Y. Arimoto, H. Seino, Y. Mizobe, K. Hashimoto, *J. Phys. Chem. B* **2003**, *107*, 11571–11574.

[102] E. Chelebaeva, J. Larionova, Y. Guari, R. A. S. Ferreira, L. D. Carlos, F. A. Almeida Paz, A. Trifonov, C. Guérin, *Inorg. Chem.* **2008**, *47*, 775–777.
[103] E. Chelebaeva, J. Larionova, Y. Guari, R. A. S. Ferreira, L. D. Carlos, F. A. Almeida Paz, A. Trifonov, C. Guérin, *Inorg. Chem.* **2009**, *48*, 5983–5995.
[104] S.-L. Ma, S. Ren, Y. Ma, D.-Z. Liao, *J. Chem. Sci.* **2009**, *121*, 421–427.
[105] A.-H. Yuan, P. D. Southon, D. J. Price, C. J. Kepert, H. Zhou, W.-Y. Liu, *Eur. J. Inorg. Chem.* **2010**, 3610–3614.
[106] Y. Arimoto, S. Ohkoshi, Z. J. Zhong, H. Seino, Y. Mizobe, K. Hashimoto, *Chem. Lett.* **2002**, *31*, 832–833.
[107] H. Tokoro, K. Nakagawa, K. Nakabayashi, T. Kashiwagi, K. Hashimoto, S. Ohkoshi, *Chem. Lett.* **2009**, *38*, 338–339.
[108] J. Larionova, R. Clerac, B. Donnadieu, S. Willemin, C. Guerin, *Cryst. Growth Des.* **2003**, *3*, 267–272.
[109] F. Chang, H.-L. Sun, H.-Z. Kou, S. Gao, *Inorg. Chem. Commun.* **2002**, *5*, 660–663.
[110] D. Li, L. Zheng, X. Wang, J. Huang, S. Gao, W. Tang, *Chem. Mater.* **2003**, *15*, 2094–2098.
[111] H. Higashikawa, K. Okuda, J. Kishine, N. Masuhara, K. Inoue, *Chem. Lett.* **2007**, *36*, 1022–1023.
[112] S. Ohkoshi, Y. Arimoto, T. Hozumi, H. Seino, Y. Mizobe, K. Hashimoto, *Chem. Commun.* **2003**, 2772–2773.
[113] T. Korzeniak, K. Stadnicka, R. Pełka, M. Bałanda, K. Tomala, K. Kowalski, B. Sieklucka, *Chem. Commun.* **2005**, 2939–2941.
[114] S. L. Ma, S. Ren, Y. Ma, D. Z. Liao, *Struct. Chem.* **2009**, *20*, 145–154.
[115] Y. Wang, T.-W. Wang, H.-P. Xiao, Y.-Z. Li, Y. Song, X.-Z. You, *Chem. Eur. J.* **2009**, *15*, 7648–7655.
[116] H. Zhou, A.-H. Yuan, X.-P. Shen, Y.-Y. Chen, D. J. Price, C. J. Kepert, *Inorg. Chem. Commun.* **2007**, *10*, 940–943.
[117] Z.-X. Wang, P. Zhang, X.-F. Shen, Y. Song, X.-Z. You, K. Hashimoto, *Cryst. Growth Des.* **2006**, *6*, 2457–2462.
[118] Y.-Y. Chen, H. Zhou, X.-P. Shen, H.-F. Lu, A.-H. Yuan, *J. Mol. Struct.* **2007**, *839*, 64–68.
[119] D.-F. Li, T. Okamura, W.-Y. Sun, N. Ueyama, W.-X. Tang, *Acta Crystallogr., Sect. C* **2002**, *58*, m280–m282.
[120] D.-F. Li, S. Gao, L.-M. Zheng, W.-Y. Sun, T. Okamura, N. Ueyama, W.-X. Tang, *New J. Chem.* **2002**, *26*, 485–489.
[121] a) J. M. Herrera, A. Bleuzen, Y. Dromzee, M. Julve, F. Lloret, M. Verdaguer, *Inorg. Chem.* **2003**, *42*, 7052–7059; b) K. Imoto, D. Takahashi, Y. Tsunobuchi, W. Kosaka, M. Arai, H. Tokoro, S. Ohkoshi, *Eur. J. Inorg. Chem.* **2010**, 4079–4082.
[122] J. Lu, W. T. A. Harrison, A. J. Jacobson, *Angew. Chem.* **1995**, *107*, 2759; *Angew. Chem. Int. Ed. Engl.* **1995**, *34*, 2557–2559.
[123] J. M. Herrera, P. Franz, R. Podgajny, M. Pilkington, M. Biner, S. Decurtins, H. Stoeckli-Evans, A. Neels, R. Garde, Y. Dromzee, M. Julve, B. Sieklucka, K. Hashimoto, S. Ohkoshi, M. Verdaguer, *C. R. Chim.* **2008**, *11*, 1192–1199.
[124] W. Dong, Y.-Q. Sun, L.-N. Zhu, D.-Z. Liao, Z.-H. Jiang, S.-P. Yan, P. Cheng, *New J. Chem.* **2003**, *27*, 1760–1764.
[125] G. Rombaut, C. Mathoniere, P. Guionneau, S. Golhen, L. Ouahab, M. Verelst, P. Lecante, *Inorg. Chim. Acta* **2001**, *326*, 27–36.
[126] D. Pinkowicz, R. Podgajny, R. Pełka, W. Nitek, M. Bałanda, M. Makarewicz, M. Czapla, J. Żukrowski, C. Kapusta, D. Zając, B. Sieklucka, *Dalton Trans.* **2009**, 7771–7777.
[127] Z.-X. Wang, X.-F. Shen, J. Wang, P. Zhang, Y.-Z. Li, E. N. Nfor, Y. Song, S. Ohkoshi, K. Hashimoto, X.-Z. You, *Angew. Chem.* **2006**, *118*, 3365; *Angew. Chem. Int. Ed.* **2006**, *45*, 3287–3291.
[128] D. Matoga, M. Mikuriya, M. Handa, J. Szklarzewicz, *Chem. Lett.* **2005**, *34*, 1550–1551.
[129] a) Y. Song, S. Ohkoshi, Y. Arimoto, H. Seino, Y. Mizobe, K. Hashimoto, *Inorg. Chem.* **2003**, *42*, 1848–1856; b) T.-W. Wang, J. Wang, S. Ohkoshi, Y. Song, X.-Z. You, *Inorg. Chem.* **2010**, *49*, 7756–7763.
[130] a) S. Ohkoshi, S. Ikeda, T. Hozumi, T. Kashiwagi, K. Hashimoto, *J. Am. Chem. Soc.* **2006**, *128*, 5320–532; b) S. Ohkoshi, Y. Hamada, T. Matsuda, Y. Tsunobuchi, H. Tokoro, *Chem. Mater.* **2008**, *20*, 3048–3054.
[131] F.-T. Chen, D.-F. Li, S. Gao, X.-Y. Wang, Y.-Z. Li, L.-M. Zheng, W.-X. Tang, *Dalton Trans.* **2003**, 3283–3287.
[132] Z.-X. Wang, X.-L. Li, B.-L. Liu, H. Tokoro, P. Zhang, Y. Song, S. Ohkoshi, K. Hashimoto, X.-Z. You, *Dalton Trans.* **2008**, 2103–2106.
[133] R. Podgajny, M. Bałanda, M. Sikora, M. Borowiec, L. Spałek, C. Kapusta, B. Sieklucka, *Dalton Trans.* **2006**, 2801–2809.
[134] S. Tanase, F. Prins, J. M. M. Smits, R. de Gelder, *CrystEngComm* **2006**, *8*, 863–865.
[135] H. Zhou, A.-H. Yuan, S.-Y. Qian, Y. Song, G.-W. Diao, *Inorg. Chem.* **2010**, *49*, 5971–5976.
[136] J. Qian, H. Yoshikawa, J. Zhang, H. Zhao, K. Awaga, C. Zhang, *Cryst. Growth Des.* **2009**, *9*, 5351–5355.
[137] W. Kosaka, T. Nuida, K. Hashimoto, S. Ohkoshi, *Bull. Chem. Soc. Jpn.* **2007**, *80*, 960–962.
[138] W. Kosaka, K. Hashimoto, S. Ohkoshi, *Bull. Chem. Soc. Jpn.* **2008**, *81*, 992–994.
[139] Y. Tsunobuchi, W. Kosaka, T. Nuida, S. Ohkoshi, *CrystEngComm* **2009**, *11*, 2051–2053.
[140] T. Kashiwagi, S. Ohkoshi, H. Seino, Y. Mizobe, K. Hashimoto, *J. Am. Chem. Soc.* **2004**, *126*, 5024–5025.
[141] Y. Tsunobuchi, K. Hashimoto, M. Shiro, T. Hozumi, S. Ohkoshi, *Chem. Lett.* **2007**, *36*, 1464–1465.
[142] S. Ohkoshi, Y. Tsunobuchi, H. Takahashi, T. Hozumi, M. Shiro, K. Hashimoto, *J. Am. Chem. Soc.* **2007**, *129*, 3084–3085.
[143] O. Sato, T. Iyoda, A. Fujishima, K. Hashimoto, *Science* **1996**, *272*, 704–705.
[144] S. Ohkoshi, H. Tokoro, T. Hozumi, Y. Zhang, K. Hashimoto, C. Mathoniere, I. Bord, G. Rombaut, M. Verelst, C. Cartier dit Moulin, F. Villain, *J. Am. Chem. Soc.* **2006**, *128*, 270–277.
[145] X.-D. Ma, T. Yokoyama, T. Hozumi, K. Hashimoto, S. Ohkoshi, *Phys. Rev. B* **2005**, *72*, 094107.
[146] R. Raghunathan, S. Ramasesha, C. Mathonière, V. Marvaud, *Phys. Rev. B* **2006**, *73*, 045131.
[147] R. Raghunathan, S. Ramasesha, C. Mathoniere, V. Marvaud, *Phys. Chem. Chem. Phys.* **2008**, *10*, 5469–5474.
[148] M.-A. Arrio, J. Long, C. Cartier dit Moulin, A. Bachschmidt, V. Marvaud, A. Rogalev, C. Mathonière, F. Wilhelm, P. Saintctavit, *J. Phys. Chem. C* **2010**, *114*, 593–600.
[149] T. Yokoyama, K. Okamoto, D. Matsumura, T. Ohta, S. Ohkoshi, K. Hashimoto, *J. Synchrotron Radiat.* **2001**, *8*, 913–915.
[150] T. Yokoyama, K. Okamoto, T. Ohta, S. Ohkoshi, K. Hashimoto, *Phys. Rev. B* **2002**, *65*, 064438.
[151] R. Le Bris, C. Mathoniere, J.-F. Letard, *Chem. Phys. Lett.* **2006**, *426*, 380–386.
[152] T. Mahfoud, G. Molnar, S. Bonhommeau, S. Cobo, L. Salmon, P. Demont, H. Tokoro, S. Ohkoshi, K. Boukheddaden, A. Bousseksou, *J. Am. Chem. Soc.* **2009**, *131*, 15049–15054.
[153] M. Zieliński, P. Tracz, R. Podgajny, R. Pełka, M. Bałanda, T. Wasiutyński, B. Sieklucka, *Acta Phys. Polonica A* **2007**, *112*, S183.
[154] T. Korzeniak, C. Mathoniere, A. Kaiba, P. Guionneau, M. Kozieł, B. Sieklucka, *Inorg. Chim. Acta* **2008**, *361*, 3500.
[155] M. Kozieł, R. Podgajny, R. Kania, R. Lebris, C. Mathoniere, K. Lewiński, K. Kruczała, M. Rams, C. Labrugere, A. Bousseksou, B. Sieklucka, *Inorg. Chem.* **2010**, *49*, 2765–2772.
[156] L. Néel, *Ann. Phys. (Leipzig)* **1948**, *3*, 137–198.
[157] S. Ohkoshi, T. Iyoda, A. Fujishima, K. Hashimoto, *Phys. Rev. B* **1997**, *56*, 11642–11652.
[158] O. Kahn, *Molecular Magnetism*, VCH Publishers, New York, **1993**, ch. 8.4.2.

[159] M. Verdaguer, G. Girolami, "Magnetic Prussian Blue Analogs" in *Magnetism: Molecules to Materials V* (Eds.: J. S. Miller, M. Drillon), Wiley-VCH Verlag GmbH & Co. KGaA, Weinheim, **2004**, ch. 9.
[160] T. Hozumi, T. Nuida, K. Hashimoto, S. Ohkoshi, *Cryst. Growth Des.* **2006**, *6*, 1736–1737.
[161] K. Nakagawa, H. Tokoro, S. Ohkoshi, *Inorg. Chem.* **2008**, *47*, 10810–10812.
[162] M. Arai, W. Kosaka, T. Matsuda, S. Ohkoshi, *Angew. Chem.* **2008**, *120*, 6991; *Angew. Chem. Int. Ed.* **2008**, *47*, 6885–6887.
[163] B. Sieklucka, R. Podgajny, D. Pinkowicz, B. Nowicka, T. Korzeniak, M. Bałanda, T. Wasiutyński, R. Pełka, M. Makarewicz, M. Czapla, M. Rams, B. Gaweł, W. Łasocha, *CrystEngComm* **2009**, *11*, 2032–2039.
[164] W. Kosaka, K. Imoto, Y. Tsunobuchi, S. Ohkoshi, *Inorg. Chem.* **2009**, *48*, 4604–4606.

Received: October 3, 2010
Published Online: December 20, 2010

